



UNIVERSITY OF LEEDS

This is a repository copy of *A methodology for Raman characterisation of MoDTC tribofilms and its application in investigating the influence of surface chemistry on friction performance of MoDTC lubricants*.

White Rose Research Online URL for this paper:  
<http://eprints.whiterose.ac.uk/87218/>

Version: Accepted Version

---

**Article:**

Khaemba, DN, Neville, A and Morina, A (2015) A methodology for Raman characterisation of MoDTC tribofilms and its application in investigating the influence of surface chemistry on friction performance of MoDTC lubricants. *Tribology Letters*, 59 (3). 38. ISSN 1023-8883

<https://doi.org/10.1007/s11249-015-0566-6>

---

**Reuse**

Unless indicated otherwise, fulltext items are protected by copyright with all rights reserved. The copyright exception in section 29 of the Copyright, Designs and Patents Act 1988 allows the making of a single copy solely for the purpose of non-commercial research or private study within the limits of fair dealing. The publisher or other rights-holder may allow further reproduction and re-use of this version - refer to the White Rose Research Online record for this item. Where records identify the publisher as the copyright holder, users can verify any specific terms of use on the publisher's website.

**Takedown**

If you consider content in White Rose Research Online to be in breach of UK law, please notify us by emailing [eprints@whiterose.ac.uk](mailto:eprints@whiterose.ac.uk) including the URL of the record and the reason for the withdrawal request.



[eprints@whiterose.ac.uk](mailto:eprints@whiterose.ac.uk)  
<https://eprints.whiterose.ac.uk/>

# **A methodology for Raman characterisation of MoDTC tribofilms and its application in investigating the influence of surface chemistry on friction performance of MoDTC lubricants**

\*Doris N Khaemba, Anne Neville, Ardian Morina

Institute of Functional Surfaces (iFS), School of Mechanical Engineering, University of Leeds, LS2 9JT, Leeds, UK.

\* Corresponding author: d.n.khaemba@leeds.ac.uk, Tel: +44 01133432179

## **Abstract**

In this study, Raman spectroscopy has been employed to understand the influence of surface chemistry on friction in a tribocontact. Tribotests were conducted using molybdenum dialkyldithiocarbamate (MoDTC) lubricant in a steel/steel sliding contact. Firstly, surface chemistry in the high friction regime, at the beginning of the test, and in the low friction regime, after longer test duration is investigated. Secondly, the influence of temperature on the surface chemistry of the resulting wear scars is investigated. Results show that at the beginning of tribotests with MoDTC lubricant, iron oxides are formed in the tribocontact which result in high friction. At longer test durations, adsorbed MoDTC on the ferrous surface decomposes to form MoS<sub>2</sub> and low friction is observed. Surface chemistry at the tribocontact has been found to vary depending on the test temperature. At high temperatures, MoS<sub>2</sub> is formed which provides friction reduction while at low temperatures, molybdenum oxide and amorphous sulphur-rich molybdenum (MoS<sub>x</sub>) compounds are formed which do not provide friction reduction. Furthermore, it has been shown that MoS<sub>2</sub> formed within the tribocontact at high temperatures has a slightly disordered crystal structure as a result of tribological processes.

## **Keywords**

Boundary lubrication; MoS<sub>2</sub>; MoS<sub>x</sub>; Raman spectroscopy; MoDTC tribofilms; Surface chemistry;

## 1 Introduction

It is estimated that 21.5% of fuel energy in passenger cars is used to move the car while 28% is used to overcome friction losses in the engine, transmission and tires [1]. Friction reduction by about 18% by employing technological advances in surface coatings, texturing and the use of novel additives would lead to more than 37% reduction in fuel consumption as well as economic savings and reduction in CO<sub>2</sub> emission [1]. About 10% of friction losses in the piston assembly occur in the boundary lubrication regime where metal-metal contact is present [2]. Lubrication in this regime is achieved by using lubricants containing chemically active additives which react with the surfaces forming tribofilms which provide friction and wear reduction due to their physicochemical properties.

Molybdenum dialkyl dithiocarbamate (MoDTC) is an additive added in engine oil mainly as a friction modifier. MoDTC reduces friction by degradation of the molecule to form discrete MoS<sub>2</sub> sheets of about 10 nm - 20 nm in diameter and 1-2 nm thick [3]. The presence of MoS<sub>2</sub> in the rubbing contact greatly reduces friction due to interlayer sliding of MoS<sub>2</sub> sheets between the sliding pair and only a few sheets are necessary for low friction to be achieved [4]. In a steel/steel sliding contact, the friction coefficient achieved in the presence of MoDTC can be as low as  $\mu=0.04$  at ambient conditions [5] and  $\mu=0.02$  in a vacuum environment [3].

Formation of MoDTC tribofilms is affected by parameters such as temperature, MoDTC concentration, the presence of antioxidants and other lubricant additives as well as contact parameters such as the stroke length, sliding speed, slide-roll ratio and surface roughness of the sliding pair which in turn affect the friction performance of the additive [6-12]. Although there is a consensus within the research community that MoDTC reduces friction by formation of MoS<sub>2</sub> within the contact region, there is still no mechanistic model that links additive chemistry in a dynamic tribological system to friction and wear performance. This is mainly because of the difficulty in monitoring surface chemistry changes at the contact region in-situ and in real-time. Real-time monitoring of surface chemistry is only possible by using in-situ analysis techniques. MoDTC tribofilms have been chemically characterised in-situ using XPS [3]. XPS requires a vacuum environment thus it cannot be used to analyse samples that have not been cleaned. Raman spectroscopy allows characterisation of MoDTC tribofilms at ambient conditions and samples can be analysed without cleaning thus

preventing loss of chemical information or alteration of the surface chemistry. This technique therefore has great potential for conducting in-situ out-of-contact analysis of MoDTC tribofilms generated in steel/steel contacts.

MoDTC tribofilms are very thin and can be damaged easily by lasers used during Raman analysis. Laser damage to the tribofilms can alter the surface chemistry giving wrong chemical interpretation of the tribofilms. For Raman spectroscopy to be successfully employed in characterisation of MoDTC and other tribofilms, it is important to ensure that suitable spectra acquisition parameters are used.

Previous Raman studies have shown that MoDTC tribofilms are composed of MoS<sub>2</sub> [13]. However there have been no studies on the chemical and physical changes that occur within these tribofilms during sliding. Friction curves obtained from tests with MoDTC lubricants show an initial high friction followed by a rapid drop to low friction after a short induction time. Chemical analysis of the tribocontact during the short period at the beginning of tribotests when friction is high and after longer test durations when friction is low would provide a better insight on the chemical changes that occur at the tribocontact during sliding.

The low friction observed when MoDTC lubricants are used has been attributed to the formation of MoS<sub>2</sub> within the tribocontact. Low friction is however not always observed, especially when tests are conducted at low additive concentrations and low temperatures. In these instances, higher friction is normally observed [9]. It is highly probable that the high friction observed could be related to the surface chemistry at the tribocontact. It is therefore important to investigate the surface chemistry during tests at low additive concentrations and low temperatures.

The objectives of this work are to (1) investigate the influence of Raman spectra acquisition parameters on spectra obtained from MoDTC tribofilms (2) investigate chemical changes that occur within the tribocontact during sliding in the presence of MoDTC lubricant (3) study the influence of temperature on surface chemistry and friction performance of MoDTC lubricants.

## **1.1 Raman spectroscopic studies on MoS<sub>2</sub>**

MoS<sub>2</sub> is a naturally-occurring crystal with a hexagonal lattice structure [14]. It is composed of separate layers; each layer consists of molybdenum atoms sandwiched between sulphur

atoms. Adjacent MoS<sub>2</sub> layers are weakly bonded via Coulombic forces [15]. When excited with electromagnetic waves at ambient conditions, molybdenum and sulphur atoms within the MoS<sub>2</sub> lattice structure vibrate both in-plane and out-of-plane. These vibration modes can be Raman active, infrared active, inactive or both Raman active and infrared active. In-plane vibration modes are E<sup>1</sup><sub>1u</sub> (infrared), E<sup>2</sup><sub>2g</sub> (Raman), E<sub>2u</sub> (inactive), E<sub>1g</sub> (Raman), E<sup>1</sup><sub>2g</sub> (Raman), E<sup>2</sup><sub>1u</sub> (Infrared) while out-of-plane vibration modes are A<sup>1</sup><sub>2u</sub> (Infrared), B<sup>2</sup><sub>2g</sub> (inactive), B<sub>1u</sub> (inactive), A<sub>1g</sub> (Raman), A<sup>2</sup><sub>2u</sub> (Infrared), B<sup>1</sup><sub>2g</sub> (inactive) [16]. First-order Raman modes are the E<sup>2</sup><sub>2g</sub>, E<sub>1g</sub>, E<sup>1</sup><sub>2g</sub> and A<sub>1g</sub> and are observed at 34 cm<sup>-1</sup>, 287 cm<sup>-1</sup>, 383 cm<sup>-1</sup> and 409 cm<sup>-1</sup>, respectively [17]. The E<sup>2</sup><sub>2g</sub> and E<sup>1</sup><sub>2g</sub> modes involve the vibration of both molybdenum and sulphur atoms while the E<sub>1g</sub> mode involves the vibration of only sulphur atoms. The A<sub>1g</sub> mode involves the vibration of sulphur atoms away from the molybdenum atom in both directions of the MoS<sub>2</sub> layer.

The E<sup>2</sup><sub>2g</sub> mode involves vibration of adjacent MoS<sub>2</sub> layers and is a relatively weak vibration compared to the other three modes [18]. The E<sub>1g</sub> mode is also a weak mode and is sensitive to the polarisation of the laser on the incident plane. This mode is intense when p-polarised light is used (i.e. the electric field of the incident laser light is parallel to the basal plane of MoS<sub>2</sub>) [18]. The orientation of the MoS<sub>2</sub> crystal also determines whether the E<sub>1g</sub> mode is observed or not. Wieting and Verble [19] showed that E<sub>1g</sub> mode was only observed when the observation plane was along the z-axis.

Of the four first-order Raman modes, the E<sup>1</sup><sub>2g</sub> and A<sub>1g</sub> modes have peaks with the highest intensities. For a given laser polarisation, the peak intensity ratio of E<sup>1</sup><sub>2g</sub> to A<sub>1g</sub> mode is dependent on the collection angle of the scattered light. Raman studies by Wang et al. [20] on a single MoS<sub>2</sub> monolayer found that the intensity of the A<sub>1g</sub> mode was highest when the angle between the incident and scattered light was at 0° (i.e. backscattering configuration) or 180° and lowest at 90° and 270° while the intensity of the E<sup>1</sup><sub>2g</sub> mode was not affected by the collection angle.

Polarisation of laser light has also been shown to affect peak intensities of MoS<sub>2</sub> first-order modes. Chen and Wang [18] found that the intensity of the A<sub>1g</sub> mode was twice that of the E<sup>1</sup><sub>2g</sub> mode using s-polarised laser (when the electric field is perpendicular to the basal plane). The intensity of both modes was comparable when p-polarised laser (electric field parallel to the plane of incidence) was used.

In addition to first-order peaks, second-order peaks are observed when laser wavelengths close to the absorption band of MoS<sub>2</sub> are used due to resonance effect. Absorption in MoS<sub>2</sub> occurs at 1.9 eV and 2.1 eV which corresponds to 652.6 nm and 590.5 nm laser wavelengths respectively [21]. Table 1 summarizes Raman peaks observed under resonance conditions and their assignments obtained from literature. Second-order peaks observed at 150 cm<sup>-1</sup> and 188 cm<sup>-1</sup> are due to a difference process and are therefore not observed at very low temperatures [18,22]. MoS<sub>2</sub> nanoparticles have been found to have additional second-order peaks which are observed at 226 cm<sup>-1</sup>, 247 cm<sup>-1</sup>, 495 cm<sup>-1</sup> and 545 cm<sup>-1</sup> [22].

Table 1. Assignment of Raman bands due to resonance Raman scattering.

Peak frequency (cm <sup>-1</sup> )	First-order	Second-order	References
34	E <sub>2g</sub> <sup>2</sup>		[18,23]
150		E <sub>2g</sub> <sup>1</sup> -LA(M)	[18,24]
188		A <sub>1g</sub> -LA(M)	[22,24]
226, 247	LA(M)		[22]
287	E <sub>1g</sub>		[17]
383	E <sub>2g</sub> <sup>1</sup>		[17,24]
408	A <sub>1g</sub>		[17,24]
422		E <sub>1u</sub> <sup>2</sup>	[24]
455, 495		2LA(M)	[18,22]
466		A <sub>1u</sub>	[22]
526, 545		E <sub>1g</sub> +LA(M)	[22,24]
567		2E <sub>1g</sub>	[18,25]
596		E <sub>2g</sub> <sup>1</sup> +LA(M)	[18,25]
641		A <sub>1g</sub> + LA(M)	[25]
750		2E <sub>2g</sub> <sup>1</sup>	[18,24]
778		A <sub>1g</sub> + E <sub>2g</sub> <sup>1</sup>	[18,25]
820		2A <sub>1g</sub>	[18,24,25]

First-order and second-order MoS<sub>2</sub> peaks have been used to study disorder in MoS<sub>2</sub> films [26] and nanoparticles [22]. It has been shown that disorder in MoS<sub>2</sub> films and size reduction in nanoparticles results in broadening of peaks. First-order peaks have been particularly useful in determining the thickness of a few MoS<sub>2</sub> layers [23,27-29]. The E<sub>2g</sub><sup>1</sup> peak has been observed to red shift while the A<sub>1g</sub> peak blue shifts from a monolayer to four layers thus the difference in peak frequency can be used as a measure for layer thickness. Furthermore, the peak width (full width at half maxima, FWHM) of the A<sub>1g</sub> mode has been found to decrease

with increase in the number of layers from two layers to about six layers. Second-order peaks have also been shown to be layer dependent [30].

MoS<sub>2</sub> peak frequencies are greatly affected by stress-induced disorder. Studies have shown that under strain the A<sub>1g</sub> and E<sup>1</sup><sub>2g</sub> peaks shift to higher wavenumbers and have pressure coefficients of 3.7 cm<sup>-1</sup>/GPa and 1.8 cm<sup>-1</sup>/GPa, respectively [31-33]. Peak frequencies and widths are also affected by temperature. At temperatures below 500 K, the A<sub>1g</sub> and E<sup>1</sup><sub>2g</sub> peaks red shift linearly with increase in temperature with first-order temperature coefficients of  $-1.23 \times 10^{-2}$  cm<sup>-1</sup>/K and  $-1.32 \times 10^{-2}$  cm<sup>-1</sup>/K, respectively [32,34-37]. The peak width also increases linearly with increase in temperature. At higher temperatures, a non-linear relationship is observed in the peak frequency shift [38]. During Raman spectra acquisition laser heating may cause the local temperature of MoS<sub>2</sub> to rise resulting in a shift in the peak frequency [39]. The A<sub>1g</sub> peak has been observed to red shift with increase in laser power at a rate of  $5.4 \pm 0.3$  cm<sup>-1</sup>/mW [34]. At very high laser powers MoS<sub>2</sub> is partially oxidised to MoO<sub>3</sub> and peaks due to the formation of the oxide are observed at 279 cm<sup>-1</sup>, 820 cm<sup>-1</sup> and 994 cm<sup>-1</sup> [24].

## 2 Experimental methodology

### 2.1 Tribotests

Tribotests were conducted using a high speed ball-on-disc tribometer under unidirectional sliding conditions. The disc was rotated against a fixed ball producing a circular wear scar on the disc. The balls and discs were made of AISI 52100 and AISI 1050 steel, respectively. The diameter of the ball bearing was 6.50 mm. The discs had an outer and inner diameter of 42 mm and 25 mm, respectively, with a thickness of 1 mm. Roughness of the balls and the discs was R<sub>a</sub>=13 nm and R<sub>a</sub>=177 nm, respectively. The Young's modulus of the balls and discs was 190-210 GPa. Tribotests were conducted using 0.6 wt% MoDTC (Mo<sub>2</sub>S<sub>2</sub>O<sub>2</sub> (CNR<sub>2</sub>)<sub>2</sub>) in Group III mineral base oil. The alkyl groups (R) in the MoDTC were a mixture of C3 and C6 alkyl chains. The additive and base oil were supplied by Total Raffinage, Solaize (France). Tests were conducted at 40°C and 100°C and disc rotating speed of 200 rpm which was equivalent to a linear speed of 0.3 m/s. The applied load was 40 N which gave an initial maximum Hertzian contact pressure of 2.12 GPa. The test duration was varied from 5 min to 3h. After tribotests, the tribopair was rinsed with heptane in an ultrasonic bath for 1 min. Wear scars formed on the discs and balls were then analysed with Raman spectroscopy.

## 2.2 Raman analysis

Raman analysis was conducted using a Renishaw InVia spectrometer (UK). The spectrometer has a spectral resolution of  $1\text{ cm}^{-1}$  and a lateral resolution of 800 nm. Raman spectra were acquired with an Olympus 50 $\times$  objective with a numerical aperture (N.A) of 0.75 in a backscattering configuration. This Raman equipment is equipped with 488 nm and 785 nm wavelength lasers operating at a maximum laser power of 10 mW and 220 mW at the source, respectively. The radius of laser spots of the 488 nm and 785 nm laser was 400 nm and 640 nm, respectively. All spectra reported here were obtained at room temperature. Peak analysis was conducted using the Renishaw WiRE program where Raman peaks were fitted with a mixed Gaussian/Lorentzian curve to determine the peak frequency, full width at half maxima (FWHM) and peak intensity.

## 3 Results

### 3.1 Influence of Raman spectra acquisition parameters

Before analysing MoDTC tribofilms a detailed study on the potential effect of Raman laser on tribofilms was conducted. This was necessary so as to ensure that the Raman spectra acquisition parameters used did not cause any laser damage to the tribofilms.

#### 3.1.1 Influence of laser wavelength

As discussed in section 1.1 above the laser wavelength can significantly alter the Raman spectra of MoS<sub>2</sub> especially when the wavelength is close to the absorption band of MoS<sub>2</sub> which occurs at 590 nm and 650 nm. The Raman equipment used in the analysis has 488 nm and 785 nm wavelength lasers which are below and above both of the absorption bands. Therefore the influence of these two laser wavelengths on spectra obtained from MoDTC tribofilms was investigated.

Figure 1 (a) shows Raman spectra obtained from MoDTC tribofilms using the 488 nm wavelength laser. The spectra from the ball and disc were similar therefore only the spectra obtained from the ball are presented here. Raman spectrum of MoS<sub>2</sub> microcrystalline powder has been included as a reference for MoS<sub>2</sub> peaks. MoS<sub>2</sub> powders were supplied by Sigma-Aldrich (UK) (99% purity) and had crystal sizes less than 2  $\mu\text{m}$ . E<sub>2g</sub><sup>1</sup> and A<sub>1g</sub> MoS<sub>2</sub> first-order modes are observed at  $380\text{ cm}^{-1}$  and  $409\text{ cm}^{-1}$ , respectively, in the spectra obtained from



wear scars on the disc in agreement with previous reports [9,13]. A broad peak is also observed around  $200\text{ cm}^{-1}$ . In  $\text{MoS}_2$  microcrystalline powder the  $E_{1g}$ ,  $E_{2g}^1$  and  $A_{1g}$  modes are observed at  $281\text{ cm}^{-1}$ ,  $374\text{ cm}^{-1}$  and  $400\text{ cm}^{-1}$ , respectively. Less intense second-order peaks are observed at  $444\text{ cm}^{-1}$ ,  $458\text{ cm}^{-1}$ ,  $555\text{ cm}^{-1}$ ,  $584\text{ cm}^{-1}$ ,  $738\text{ cm}^{-1}$  and  $812\text{ cm}^{-1}$  and are assigned to  $2LA(M)$ ,  $A_{1u}$ ,  $2E_{1g}$ ,  $E_{2g}^1 + LA(M)$ ,  $2E_{2g}^1$  and  $2A_{1g}$ , respectively [25]. It is interesting to note that these second-order peaks were observed when the  $488\text{ nm}$  laser was used although its energy is far from the  $\text{MoS}_2$  absorption band.

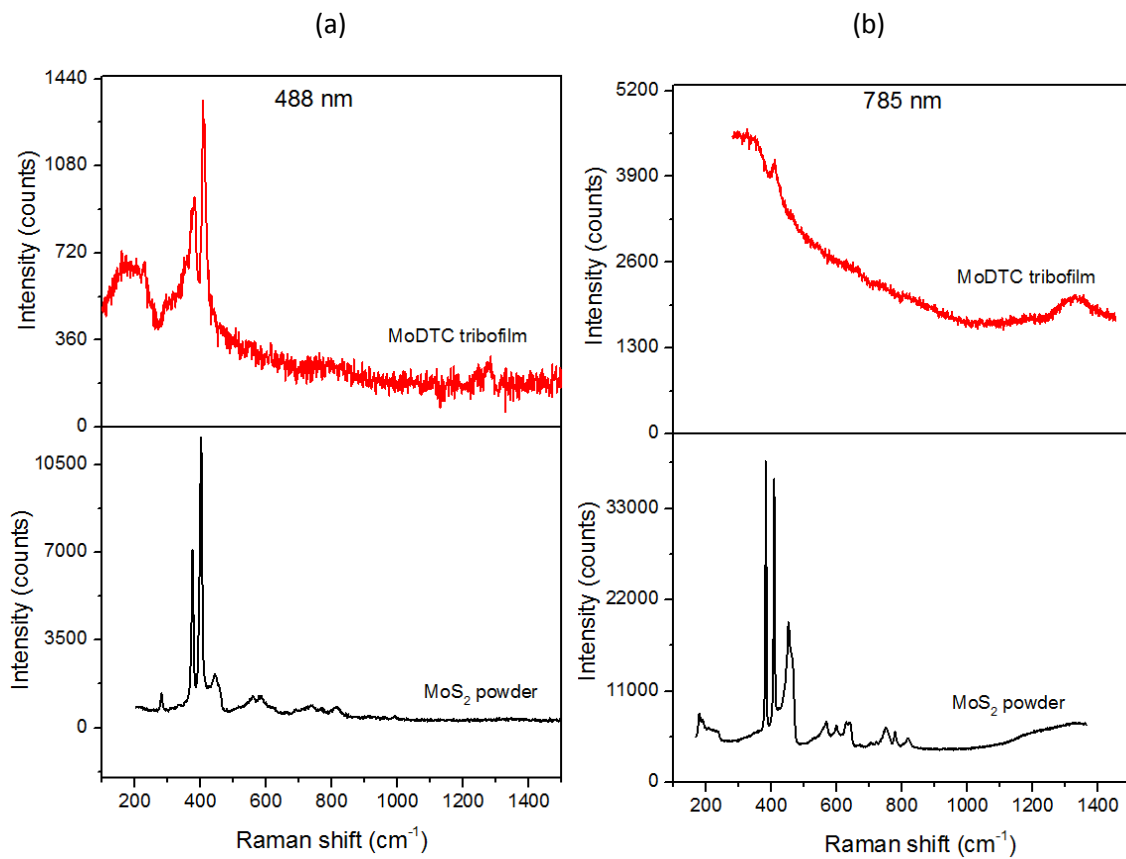


Figure 1. (a) Raman spectra of MoDTC tribofilm and  $\text{MoS}_2$  microcrystalline powder obtained using the  $488\text{ nm}$  wavelength laser at  $1\text{ mW}$  laser power,  $1\text{ s}$  exposure time,  $20$  accumulations. (b) Raman spectra of MoDTC tribofilm and  $\text{MoS}_2$  microcrystalline powder obtained using the  $785\text{ nm}$  wavelength laser at  $22\text{ mW}$  laser power,  $1\text{ s}$  exposure time,  $1$  accumulation. The tribofilms on the disc wear scar were generated after  $60\text{ min}$  sliding. The spectra are plotted on different scales.

Figure 1 (b) shows spectra obtained with the  $785\text{ nm}$  wavelength laser. First-order  $E_{2g}^1$  and  $A_{1g}$  modes are observed in  $\text{MoS}_2$  powder at  $382\text{ cm}^{-1}$  and  $407\text{ cm}^{-1}$ , respectively. Second-order peaks are also observed at  $452\text{ cm}^{-1}$ ,  $464\text{ cm}^{-1}$ ,  $562\text{ cm}^{-1}$ ,  $598\text{ cm}^{-1}$ ,  $640\text{ cm}^{-1}$ ,  $749\text{ cm}^{-1}$ ,  $778\text{ cm}^{-1}$ ,  $817\text{ cm}^{-1}$  and are assigned to  $2LA(M)$ ,  $A_{1u}$ ,  $2E_{1g}$ ,  $E_{2g}^1 + LA(M)$ ,  $A_{1g} + LA(M)$ ,  $2E_{2g}^1$ ,  $A_{1g} + E_{2g}^1$ , and  $2A_{1g}$ , respectively. The spectrum from MoDTC tribofilm does not show

any significant peaks except for the peak at  $410\text{ cm}^{-1}$  and the broad peak round  $1300\text{ cm}^{-1}$ . A high background is observed in the region where  $\text{MoS}_2$  first-order modes are expected to be observed. It was interesting to note that when the same spot showed the presence of the  $\text{MoS}_2$  peaks when probed with the 488 nm laser, no  $\text{MoS}_2$  peaks were observed when the laser was switched to 785 nm laser. Peak frequency of  $\text{MoS}_2$  first-order peaks obtained by different lasers are expected to be similar except when lasers close to the absorption band of  $\text{MoS}_2$  are used. When the laser is close to the absorption band of  $\text{MoS}_2$  additional peaks are observed and both the peak frequency and intensity of the first-order peaks can be altered. Since  $\text{MoS}_2$  first-order and second-order peaks were observed in  $\text{MoS}_2$  powder with both 785 nm and 488 nm lasers it is expected that first-order peaks should be observed in spectra from MoDTC tribofilm when probed with the 785 nm laser. However this was not the case even when laser power and exposure times were increased.

In a study by Miklozic et al. [13] MoDTC tribofilms were analysed using the 532 nm wavelength laser and  $\text{MoS}_2$  peaks were observed at  $382\text{ cm}^{-1}$  and  $412\text{ cm}^{-1}$ .  $\text{MoS}_2$  peaks have also been observed using the 632 nm wavelength laser in wear scars generated using fully formulated lubricants [40]. The reason why MoDTC tribofilms could not be characterised with the 785 nm laser is not clear yet. Since no significant peaks were observed when the 785 nm laser was used, only the 488 nm laser was used in subsequent Raman analysis.

### **3.1.2 Influence of laser power**

Thin films are easily damaged by lasers especially when high laser powers and long exposure times are used. It is therefore important to study the effect of laser power on MoDTC tribofilms for accurate chemical characterisation. The Raman equipment that was used was equipped with a microscope therefore it was possible to obtain optical images of the wear scar before and after Raman analysis in order to physically determine whether laser damage had occurred or not. Optical images of the tribopair wear scars showed that the ball wear scar was covered with a fairly even tribofilm and had a smoother topography compared to the disc wear scar which was very rough. Due to the rough nature of the disc wear scar it was difficult to observe any physical changes that occurred as a result of laser damage. On the other hand, the smooth topography of the ball wear scar allowed changes on the tribofilm due to laser damage to be observed. The effect of laser power on MoDTC tribofilms was observed to be similar on both the ball and the disc wear scars. Here, only the results from the ball wear scar

are presented since it was possible to observe changes on the tribofilm as a result of laser damage.

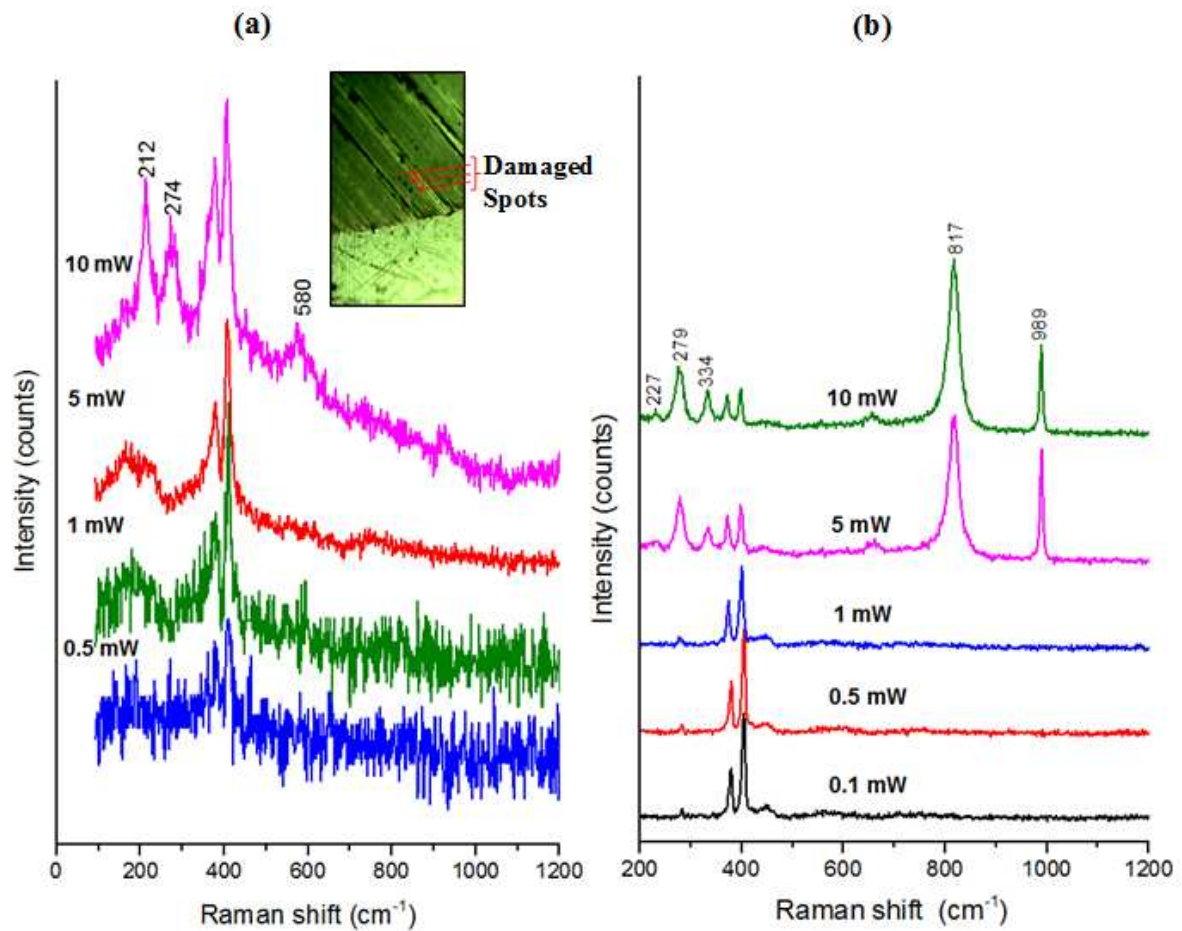


Figure 2. (a) Raman spectra of MoDTC tribofilm generated on the ball wear scar after 60 min sliding. The spectra were acquired with 488 nm wavelength laser at various laser powers. The spectra were obtained at 1s exposure time and 1 accumulation. The spectra are plotted on different scales and have been vertically shifted for clarity. Inset image shows dark burn spots on the ball wear scar after analysis at 10 mW laser power. (b) Raman spectra of MoS<sub>2</sub> microcrystalline powder obtained with 488 nm laser at various laser powers as indicated in the figure. The spectra were obtained at 1s exposure time and 1 accumulation. The spectra are plotted on the same scale and have been shifted vertically for clarity.

Figure 2 (a) shows Raman spectra from the wear scar on the ball obtained at various laser powers ranging from 0.1 mW to 10 mW. It should be noted that all spectra were obtained from the same spot starting with the lowest laser power to the highest. At laser powers less than 0.5 mW there is a very low signal-to-noise ratio (SNR) such that MoS<sub>2</sub> peaks are not clearly distinguished. The SNR increases with increase in laser power and at 5 mW laser power, the SNR is high and MoS<sub>2</sub> peaks are very distinct. At 10 mW laser power, additional

peaks are observed at  $212\text{ cm}^{-1}$ ,  $274\text{ cm}^{-1}$  and  $567\text{ cm}^{-1}$ . Also, an additional peak seems to have been formed around  $390\text{ cm}^{-1}$  and overlaps with the  $E_{2g}^1$  and  $A_{1g}$  peaks. These additional peaks were assigned to the formation of iron oxide [41]. The analysed region was observed to have developed dark spots after analysis with 10 mW laser power as seen in the inset image in Figure 2 (a). Similar spots were observed at 1 mW and 5 mW when the exposure time was increased. When the laser power was increased from 0.01 mW to 10 mW, the  $E_{2g}^1$  peak shifted from  $380\text{ cm}^{-1}$  to  $379\text{ cm}^{-1}$  while the  $A_{1g}$  peak shifted from  $410\text{ cm}^{-1}$  to  $406\text{ cm}^{-1}$ .

The effect of laser power on MoDTC tribofilms was compared to that of  $\text{MoS}_2$  microcrystalline powder. Figure 2 (b) shows spectra obtained from  $\text{MoS}_2$  powder at various laser powers. At laser power above 1 mW,  $\text{MoS}_2$  powders are partially oxidised to  $\text{MoO}_3$  as evidenced by dark spots on the sample after analysis and the emergence of strong peaks at  $817\text{ cm}^{-1}$  and  $989\text{ cm}^{-1}$  and less intense peaks at  $227\text{ cm}^{-1}$ ,  $279\text{ cm}^{-1}$  and  $334\text{ cm}^{-1}$  [24]. Above 0.5 mW laser power the intensity of the  $\text{MoS}_2$  double peaks decreased with increase in laser powers. The spectrum obtained when the MoDTC tribofilm was damaged was very different from that of damaged  $\text{MoS}_2$  microcrystalline powder. Prominent  $\text{MoO}_3$  peaks around  $820\text{ cm}^{-1}$  and  $990\text{ cm}^{-1}$  were not observed in the tribofilm at high laser power. It was also observed that when the laser power was increased from 0.01 mW to 10 mW, the  $E_{2g}^1$  peak shifted from  $382\text{ cm}^{-1}$  to  $371\text{ cm}^{-1}$  while the  $A_{1g}$  peak shifted from  $408\text{ cm}^{-1}$  to  $398\text{ cm}^{-1}$ . Compared to MoDTC tribofilms, laser power had a greater influence on  $\text{MoS}_2$  peaks position in  $\text{MoS}_2$  powder.

Due to the sensitivity of the MoDTC tribofilm to laser damage at higher laser powers, spectra of tribofilms presented in the following sections were carried out at 1 mW laser power. To improve the SNR, 20 accumulations were obtained in each spectra acquisition. It was observed that increasing the number of accumulation did not damage the sample since burn spots were not observed on the tribofilm and no additional peaks were observed on the acquired spectra.

### 3.1.3 Influence of exposure time

To further understand the influence of lasers on MoDTC tribofilms the influence of laser exposure time at high laser power was also investigated. Figure 3 shows a spectrum obtained at 10 mW laser power at 1s and 20s exposure times. In both Raman spectra peaks are

observed at  $215\text{ cm}^{-1}$ ,  $277\text{ cm}^{-1}$ ,  $381\text{ cm}^{-1}$ ,  $407\text{ cm}^{-1}$ ,  $492\text{ cm}^{-1}$ ,  $586\text{ cm}^{-1}$ ,  $923\text{ cm}^{-1}$  and  $1278\text{ cm}^{-1}$ . The peaks at  $381\text{ cm}^{-1}$  and  $407\text{ cm}^{-1}$  are assigned to  $\text{MoS}_2$  vibration modes. The intensity of the  $212\text{ cm}^{-1}$  and  $274\text{ cm}^{-1}$  peaks in the spectrum obtained at 20s exposure time has significantly increased in relation to  $\text{MoS}_2$  peaks compared to peaks in the spectrum obtained at 1s exposure time. As mentioned earlier, at 10 mW laser power it was observed that a peak emerged in the region where  $\text{MoS}_2$  peaks are observed peaks. At 20s exposure time, the intensity of this peak (around  $390\text{ cm}^{-1}$ ) was also seen to increase such that it almost overlaps with  $\text{MoS}_2$  peaks. At longer exposure times the intensity of this peak increased and completely overlapped with the  $\text{MoS}_2$  peaks resulting in a broad single peak such that the  $\text{MoS}_2$  double peak could not be distinguished from the spectrum. It is noteworthy to mention that  $\text{MoS}_2$  in MoDTC tribofilm was not partially oxidised to  $\text{MoO}_3$  even with increased laser power and exposure time. The peaks observed at  $215\text{ cm}^{-1}$ ,  $277\text{ cm}^{-1}$ ,  $586\text{ cm}^{-1}$  and  $1278\text{ cm}^{-1}$  are believed to be due to formation of iron oxide within the tribofilm at high laser powers.

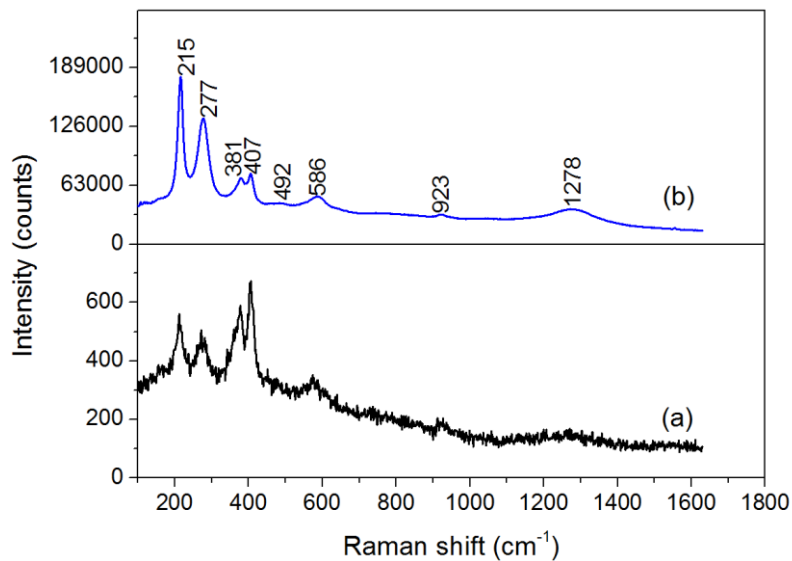


Figure 3. Raman spectra of MoDTC tribofilm on the ball wear scar obtained at 10 mW laser power at (a) 1s and (b) 20s exposure time.

### 3.1.4 Influence of laser polarisation

Raman spectra obtained from  $\text{MoS}_2$  crystals are greatly influenced by the polarisation of the laser used due to crystal lattice layer structure. Figure 4 shows spectra obtained from the same spot within a wear scar generated on a disc after tests with MoDTC lubricant. The spectra were obtained using three laser polarisations: circular, normal and orthogonal. In all the spectra,  $\text{MoS}_2$   $E_{2g}^1$  and  $A_{1g}$  peaks were observed at  $380\text{ cm}^{-1}$  and  $410\text{ cm}^{-1}$ , respectively.

Although there were no differences in the peak intensities, slight differences in the  $A_{1g}/E_{2g}^1$  peak intensity ratio were observed. The  $A_{1g}/E_{2g}^1$  ratio was 1.54, 2.14 and 1.90 for circular, normal (s-) and orthogonal (p-) polarisation, respectively. Raman spectra presented in this study were obtained using the normal polarisation.

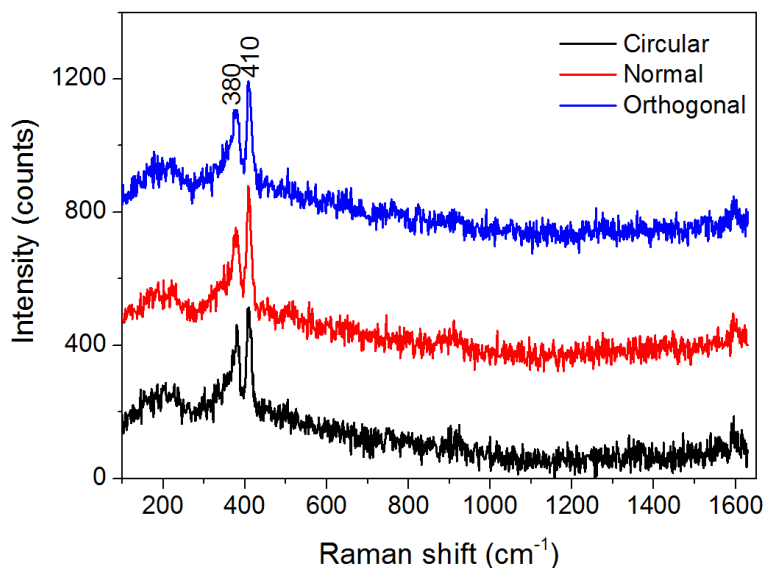


Figure 4. Raman spectra obtained from MoDTC tribofilm on the ball wear scar at different laser polarisation. Spectra were obtained at 1 mW, 1s exposure time, 20 accumulations.

### 3.2 Raman analysis: Surface chemistry at the tribocontact

To investigate changes in surface chemistry that occur within the tribocontact during tests with MoDTC lubricants, tribotests were carried at various times and the resulting wear scars were analysed. All the tests were identical and were conducted using 0.6 wt% MoDTC at 40 N (2.12 GPa), 200 rpm (0.3 m/s), 100°C. The only difference in the tests was the test duration. Tests were stopped at various rubbing times; 5 min, 20 min, 40 min, 60 min, 80 min, 100 min, and 134 min so that the chemical composition of the tribofilm in the wear scars could be monitored.

Figure 5 (b) shows the friction curve obtained in the test with MoDTC lubricant. For comparison, the friction curve of the test with mineral base oil is also presented in Figure 5 (a). In tests with mineral base oil, friction coefficient was high ( $\mu=0.13-0.15$ ) during the test. In tests with MoDTC, high friction coefficient of about  $\mu=0.15$  was observed at the beginning of the test which lasted for about 10 minutes followed by a rapid drop to lower values of  $\mu=0.06$ . The friction then gradually increased reaching steady values of about  $\mu=0.07$ . This

friction behaviour of MoDTC has been observed in other studies [5,9,13] and it has been proposed that the behaviour is as a result of an autocatalytic reaction of MoDTC [9]. With the exception of the 5 minutes test, all tests with MoDTC showed the friction drop to low friction values.

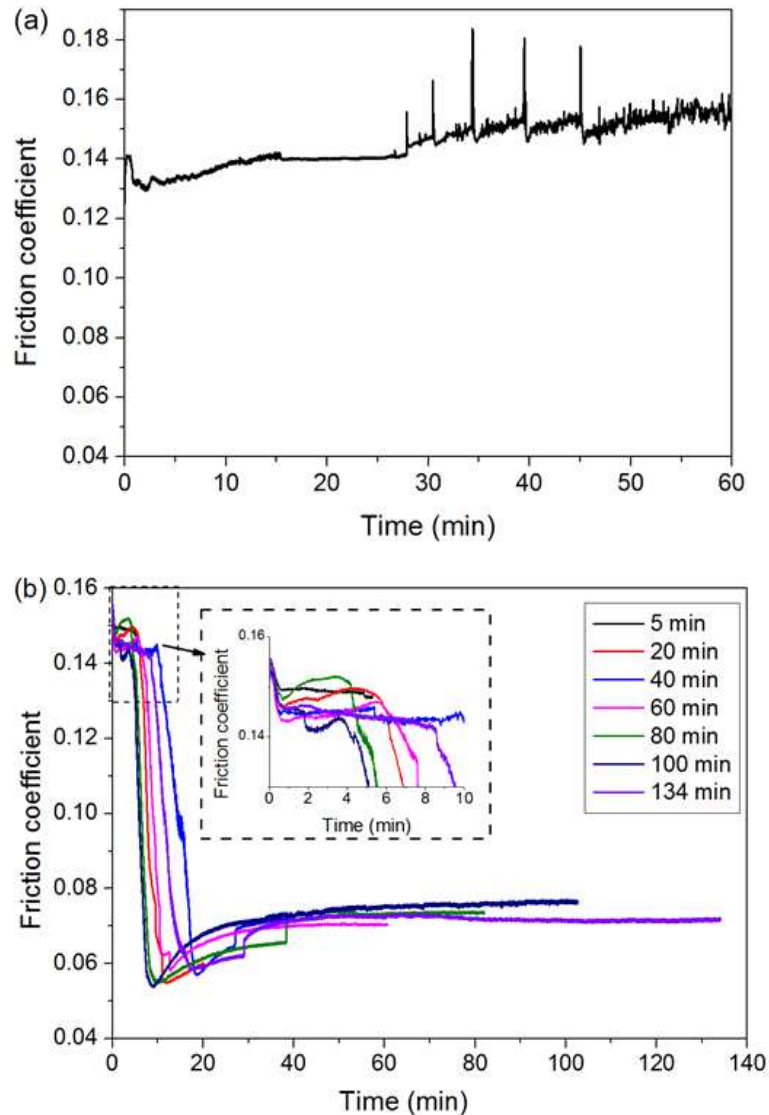


Figure 5. (a) Friction curve during test with mineral base oil. (b) Friction curve during tests with 0.6 wt% MoDTC. The test was stopped at different rubbing times as indicated. All tests were conducted at 40N (2.12 GPa pressure), 0.3 m/s, 100°C.

Figure 6 shows optical images of wear scar formed after tests with base oil and MoDTC. Roughness ( $R_a$ ) of the disc after the test with base oil was 0.110  $\mu\text{m}$ . Roughness ( $R_a$ ) of the disc after 5 minutes and 134 minutes test with MoDTC was 0.177  $\mu\text{m}$  and 0.248  $\mu\text{m}$ , respectively.

To better understand how surface chemistry affects the friction behaviour of MoDTC at short and long rubbing times, Raman analysis was carried out on the wear scars generated on the tribopair before and after the friction drop. Raman analysis was carried out on the wear scars before and after rinsing with heptane. Raman spectra obtained from both rinsed and unrinsed samples were similar. The only difference was that spectra from unrinsed samples showed peaks from the mineral base oil shown in Figure 9 (b). Unlike vacuum based techniques, unrinsed surfaces can be characterised by Raman spectroscopy. With the current trend to utilise in-situ/in-lubro techniques in tribological studies, Raman spectroscopy shows great potential as a suitable technique for analysing lubricated contacts. In section 3.2.1 and 3.2.2 Raman results from the rinsed samples is presented.

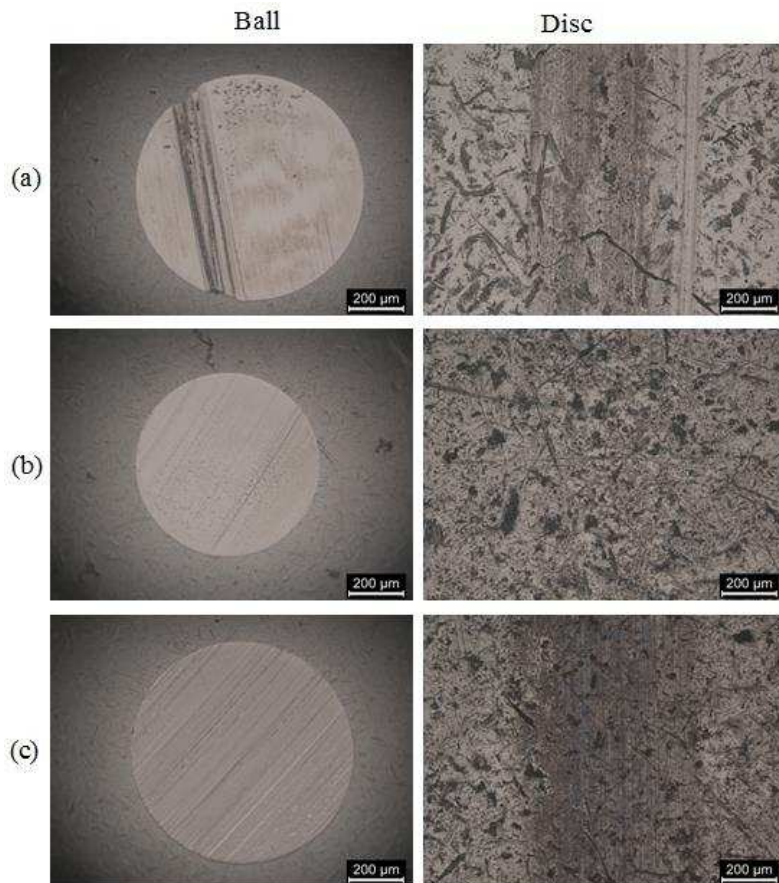


Figure 6. Optical images of the balls and discs showing wear scars generated after tribotests. (a) 60 min test with mineral base oil (b) 5 min test with MoDTC lubricant (c) 134 min test with MoDTC lubricant



### 3.2.1 Initial high friction region

Figure 7 (a) shows a typical Raman spectrum obtained from wear scars after tests with base oil. The peaks observed at  $218\text{ cm}^{-1}$ ,  $291\text{ cm}^{-1}$ ,  $404\text{ cm}^{-1}$  and  $605\text{ cm}^{-1}$  are attributed to the formation of  $\text{Fe}_2\text{O}_3$  while the peak at  $670\text{ cm}^{-1}$  is due to formation of  $\text{Fe}_3\text{O}_4$  [41]. Figure 7 (b) shows a typical Raman spectrum obtained from tribopair wear scars after 5 minutes test with MoDTC lubricant. The spectrum is similar to that observed in tests with base oil and mainly shows the presence of iron oxides. The peaks around  $1360\text{ cm}^{-1}$  and  $1590\text{ cm}^{-1}$  are attributed to formation of amorphous carbon [42]. The presence of iron oxide has also been observed in previous MoDTC studies [9]. The presence of iron oxides and absence of  $\text{MoS}_2$  explains the high friction observed in the initial stages of the test with MoDTC.

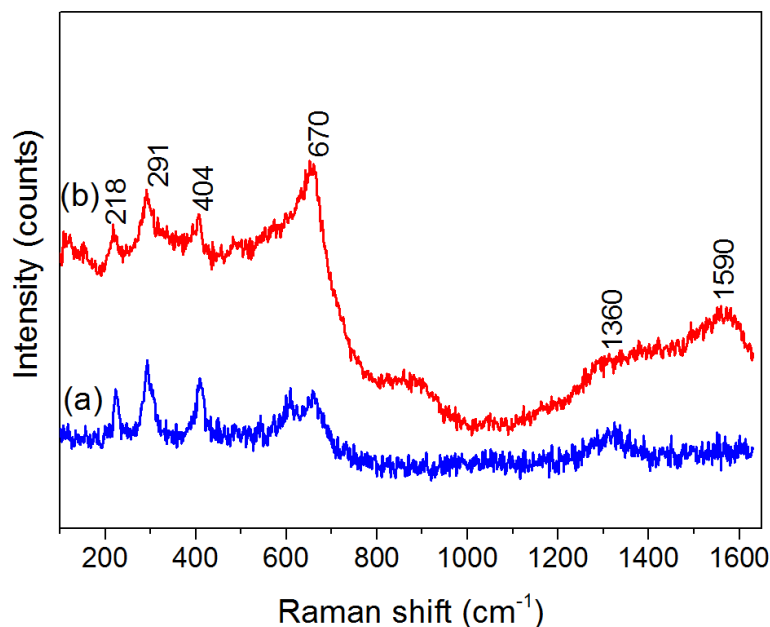


Figure 7. Raman spectra obtained from tribopair wear scars. (a) After 60 min test with mineral base oil (b) after 5 min test with MoDTC lubricant. Spectra were obtained at 1 mW laser power, 1s exposure time, 20 accumulation.

### 3.2.2 Steady low friction region

Figure 8 (a) and (b) shows representative spectra obtained for ball and disc wear scar after long test durations where friction drop to lower friction values was observed. First-order  $\text{MoS}_2$  peaks due to  $E_{2g}^1$  and  $A_{1g}$  modes were observed at  $379\text{ cm}^{-1}$  and  $409\text{ cm}^{-1}$  from spectra obtained from the tribopair wear scars. It should be highlighted that tribofilms formed on the ball and disc wear scars are very patchy in nature, therefore Raman spectra obtained from the tribofilms vary from spot-to-spot with regard to  $\text{MoS}_2$  peak intensity. Map analysis of the

wear scars where 384 spectra were obtained from areas measuring  $20\ \mu\text{m} \times 20\ \mu\text{m}$  showed that the average intensity of  $\text{MoS}_2$  peaks increased with rubbing time. This could be due to an increase in  $\text{MoS}_2$  crystallinity,  $\text{MoS}_2$  concentration or  $\text{MoDTC}$  tribofilm thickness with rubbing time. There were no significant changes in  $\text{MoS}_2$  peak frequency and peak width in spectra obtained from wear scars generated at the different test durations. Besides  $\text{MoS}_2$  peaks, broad peaks at  $1411\ \text{cm}^{-1}$  and  $1581\ \text{cm}^{-1}$  assigned to the formation of amorphous carbon were observed. A broad peak was also observed around  $200\ \text{cm}^{-1}$ . This broad peak has also been observed in sputtered and plasma laser deposited (PLD)  $\text{MoS}_2$  films where it was proposed that the broad peak was as a result of crystalline disorder in the  $\text{MoS}_2$  structure [26]. Occurrence of crystalline disorder of  $\text{MoS}_2$  in tribofilms is highly probable under tribological conditions since  $\text{MoS}_2$  nanocrystals formed in the tribofilms are subjected to stress-induced disorder. The peaks observed at  $920\ \text{cm}^{-1}$ ,  $1164\ \text{cm}^{-1}$ ,  $1240\ \text{cm}^{-1}$ ,  $1278\ \text{cm}^{-1}$ ,  $1533\ \text{cm}^{-1}$ , and  $1594\ \text{cm}^{-1}$  were from the adhesive used to attach samples on glass slides during analysis. It was noted that  $\text{MoO}_3$  did not form in the wear scars due to prolonged rubbing. It was concluded that low friction observed at longer test durations is attributed to the presence of  $\text{MoS}_2$  within the tribocontact.

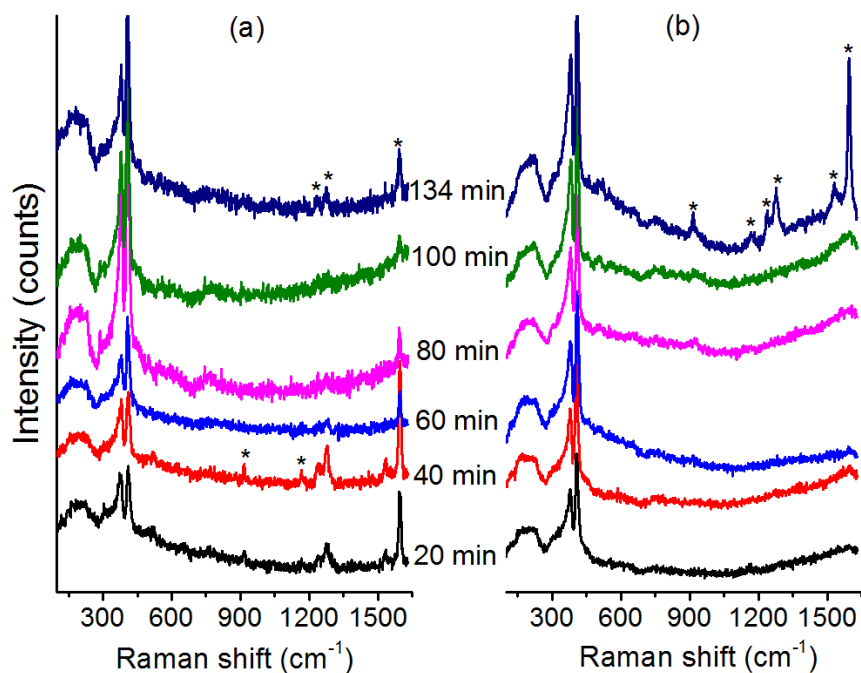


Figure 8. Raman spectra obtained from (a) ball and (b) disc wear scars generated at various test durations. All spectra were obtained using 1 mW laser power, 1s exposure time and 20 accumulations.

### 3.2.3 Raman analysis of MoDTC wear debris

After tribotests with MoDTC lubricant, at both short and long test durations, brown wear debris were observed in regions close to the wear track on the disc and were easily removed by rinsing with heptane. To study the chemical nature of the wear debris a test was conducted for 6h using 0.5 wt% MoDTC at 80°C. After tribotests, the lubricant was removed from the steel bath using a syringe and the remaining oil on the disc surface was drained off by spinning the disc at high speeds for a few minutes. The unrinsed disc was then analysed using Raman spectroscopy. The optical image in Figure 9 (a) shows wear debris on the unrinsed disc. Figure 9 (b) shows a spectrum obtained from the wear debris on the disc. MoS<sub>2</sub> peaks are observed at 379 cm<sup>-1</sup> and 411 cm<sup>-1</sup>. The presence of MoS<sub>2</sub> in the wear debris is in agreement with high resolution TEM images obtained from wear debris after tests with MoDTC lubricant [3]. A broad peak is observed at 200 cm<sup>-1</sup>. Additional peaks are also observed at 512 cm<sup>-1</sup> and 556 cm<sup>-1</sup>, these peaks are attributed to  $\nu(\text{S-S})$  vibrations [43]. Peaks at 1301 cm<sup>-1</sup> and 1444 cm<sup>-1</sup> are from the mineral base oil. Figure 9 (c) shows optical images of the tribopair after 6h test. Roughness (R<sub>a</sub>) values of wear scars on the ball and disc were 0.06  $\mu\text{m}$  and 0.269  $\mu\text{m}$ , respectively.

MoDTC thermal films were generated on the steel discs by placing the discs in a beaker containing MoDTC lubricant heated at 100°C for 3h. Raman analysis of MoDTC thermal film did not show the presence of MoS<sub>2</sub>. This shows that at 100°C, MoDTC does not decompose to form MoS<sub>2</sub> form on the steel discs and that mechanical rubbing is necessary for formation of MoS<sub>2</sub>. Therefore MoS<sub>2</sub> present in the debris is due to wear of MoDTC tribofilm and not thermal decomposition of MoDTC on the steel disc. Further evidence that MoS<sub>2</sub> in the wear debris is due to wear of MoDTC tribofilm was obtained by conducting a detailed analysis of MoS<sub>2</sub> peaks. This is discussed in greater detail in section 3.4. In summary, the E<sub>2g</sub><sup>1</sup> peak from MoS<sub>2</sub> in the wear debris and on the wear scar was found to be asymmetrical indicating stress-induced disorder in MoS<sub>2</sub> crystal structure. Stress-induced disorder in the MoS<sub>2</sub> crystal structure can only occur during tribotests since MoS<sub>2</sub> which has not been subjected to tribotests does not show asymmetry in the E<sub>2g</sub><sup>1</sup> peak.

It should however be noted that wear of the rubbing surfaces mostly occurs during the initial stages of the test (running-in process) generating wear scars. MoDTC tribofilms are then formed on the generated wear scars. The formed tribofilms are patchy in nature thus some regions of the wear scar are uncovered. During the test both the tribofilm and substrate are

continuously being worn. However, the steel substrate does not have a Raman signal therefore is not possible to detect the substrate in the wear debris. Only MoS<sub>2</sub> from the worn MoDTC tribofilm is detected in the wear debris.

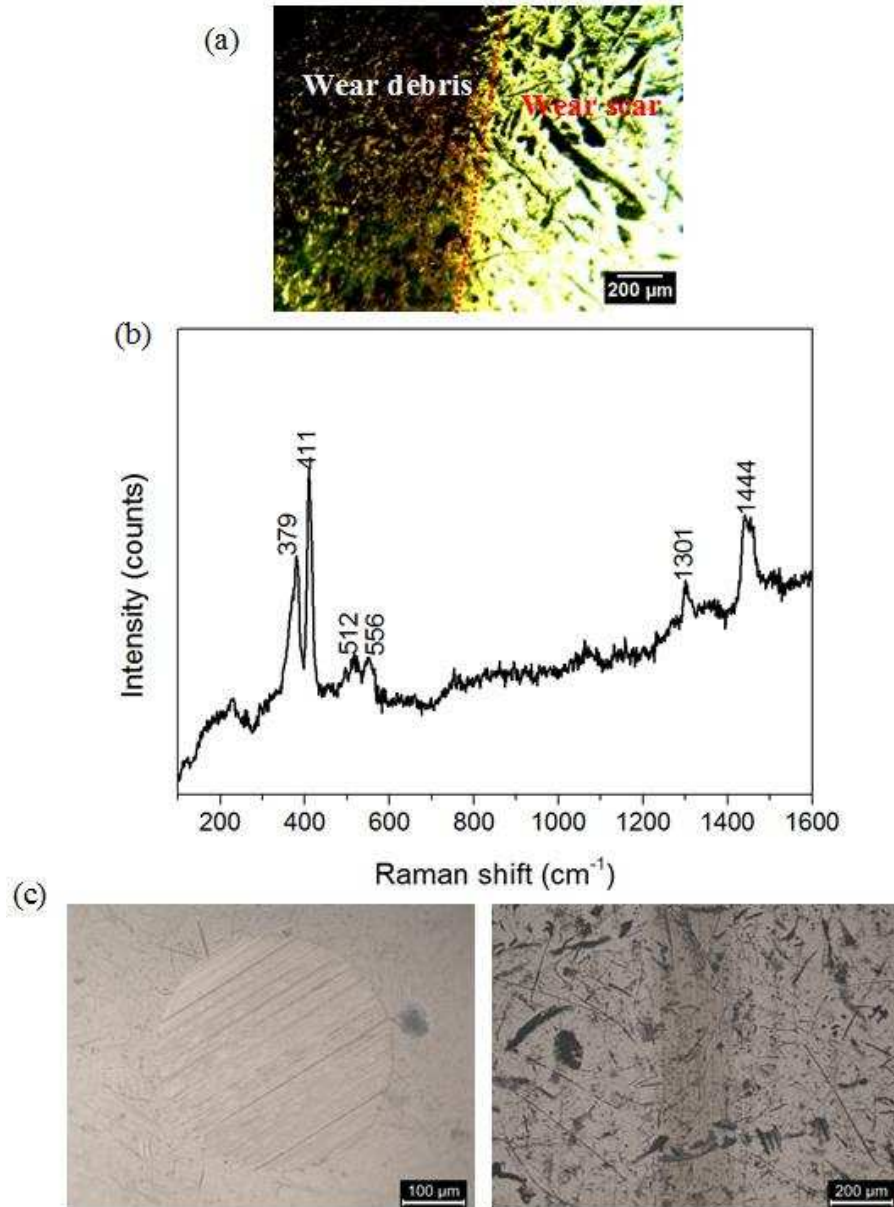


Figure 9. (a) Optical image showing wear debris on the disc after a 6h test. (b) Raman spectrum obtained from the wear debris. The spectrum was obtained using 1 mW, 1s exposure time, 20 accumulations. (c) Optical images of the ball and disc after tests showing the generated wear scar. The test was carried out using 0.5 wt% MoDTC at 200 rpm, 80°C, 1.7 GPa

### 3.3 Raman analysis: Influence of temperature on surface chemistry

From previous studies it has been shown that temperature is one of the main factors that affect the friction performance of MoDTC [9]. Graham et al. [9] showed that friction decreased with increase in temperature. Low friction observed at high temperatures was attributed to the formation of MoS<sub>2</sub> in the wear scar. The chemical nature of MoDTC decomposition product during tests at low temperatures has not been extensively investigated. Therefore tests at lower temperatures (40°C) than those presented in section 3.1.4 above (100°C) were conducted and the generated wear scars were analysed so as to have a better understanding of the surface chemistry and how it affects friction. Tribotests were conducted in the ball-on-disc tribometer using 0.6 wt% MoDTC at 2.12 GPa, 200 rpm (0.3m/s), 40°C for 3h.

Figure 10 shows the friction curve obtained in tests conducted at 40°C and 100°C. The friction behaviour in the test at low temperature is similar to that observed at high temperature, high friction at the beginning of the test followed by a rapid drop to low steady values. However, the friction coefficient at steady state is high ( $\mu=0.10$ ) compared to the test conducted at 100°C ( $\mu=0.07$ ).

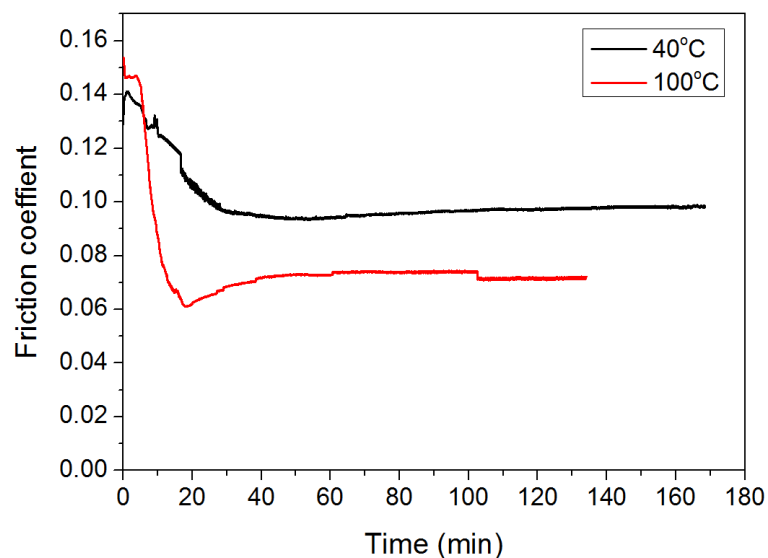


Figure 10. Friction curves of tests conducted at 40°C and 100°C.

Figure 11 (a) and (b) show optical images of ball and disc after tests at 40°C. Roughness ( $R_a$ ) value of the wear scars on the ball and disc were 0.061  $\mu\text{m}$  and 0.106  $\mu\text{m}$ , respectively. Raman analysis was conducted on different regions within the wear scars. A few

representative spectra are shown in Figure 12. Spectra obtained from different regions varied greatly. In some regions, two broad peaks are observed in the regions 100-600  $\text{cm}^{-1}$  and 600-1000  $\text{cm}^{-1}$ . The broad peak at the lower wavenumber overlaps with the  $\text{MoS}_2$  double peak although the separation between the  $E_{2g}^1$  and  $A_{1g}$  peak is clearly observed at 400  $\text{cm}^{-1}$ . The broad peak at 100-600  $\text{cm}^{-1}$  could be assigned to the formation of amorphous sulphur-rich molybdenum,  $\text{MoS}_x$  ( $x > 2$ ) [44]. The broad peak from 800  $\text{cm}^{-1}$  to 1000  $\text{cm}^{-1}$  was assigned to  $\nu(\text{Mo}=\text{O})$  vibration in molybdenum oxide species. The exact nature of the molybdenum oxide species is currently under investigation and the results will be published soon. In other regions,  $\text{MoS}_2$  peaks were clearly observed at 381  $\text{cm}^{-1}$  and 413  $\text{cm}^{-1}$ .  $\text{Fe}_3\text{O}_4$  peak was also observed at 670  $\text{cm}^{-1}$  as well as  $\nu(\text{S}-\text{S})$  vibration at 520  $\text{cm}^{-1}$ .

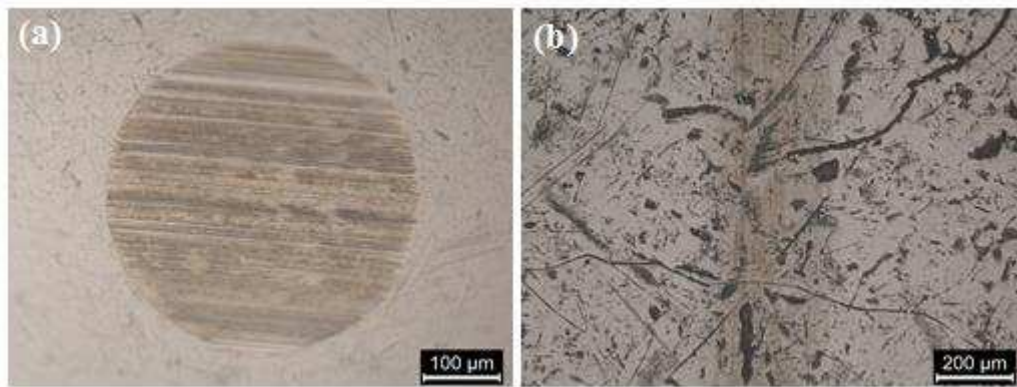


Figure 11. Optical image of the (a) ball and (b) disc wear scar after test carried out at 40°C.

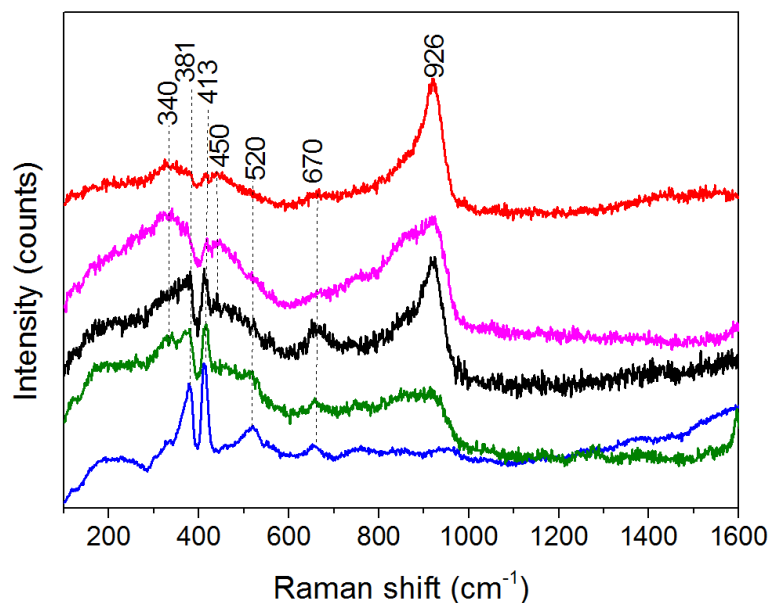


Figure 12. Raman spectra obtained from the ball wear scar after tests at 40°C.

The spectra observed from tests at 40°C are quite different from spectra obtained from tests carried out at 100°C. In tests carried out high temperatures, only MoS<sub>2</sub> was observed in the wear scars while in tests carried out at low temperatures MoS<sub>2</sub>, amorphous sulphur-rich molybdenum and molybdenum oxide species were formed. Relating the surface chemistry of the wear scars to the friction it can be concluded that the high friction coefficient values obtained in tests carried out at low temperatures was a result of formation of molybdenum oxide species and amorphous molybdenum sulphide.

### **3.4 First-order MoS<sub>2</sub> Raman modes in MoDTC tribofilms**

#### **3.4.1 MoS<sub>2</sub> Raman peak broadening and asymmetry**

Raman analysis of MoDTC tribofilms generated at high temperatures revealed slight differences in the MoS<sub>2</sub> peaks compared to microcrystalline MoS<sub>2</sub> powder. Figure 13 shows spectra of MoS<sub>2</sub> powder, MoDTC tribofilm and MoDTC wear debris in the region 300 cm<sup>-1</sup> to 450 cm<sup>-1</sup> where MoS<sub>2</sub> first-order E<sub>2g</sub><sup>1</sup> and A<sub>1g</sub> peaks are observed. The three spectra were obtained at similar acquisition parameters (i.e. 1 mW, 1s exposure time, 20 accumulation). The E<sub>2g</sub><sup>1</sup> peak in the tribofilm and wear debris was observed to be very broad and asymmetrical compared to that of MoS<sub>2</sub> powder which was narrow and symmetrical. When the two MoS<sub>2</sub> peaks were fitted with Gaussian curves it was observed that the E<sub>2g</sub><sup>1</sup> peak in the tribofilms and wear debris was fitted better with two curves, the first curve was a very broad curve at around 365 cm<sup>-1</sup> and the second at 380 cm<sup>-1</sup>. Peak information of the MoS<sub>2</sub> peaks is shown in Table 2 where values for E<sub>2g</sub><sup>1</sup> peak of the tribofilms are taken from the second curve fit.

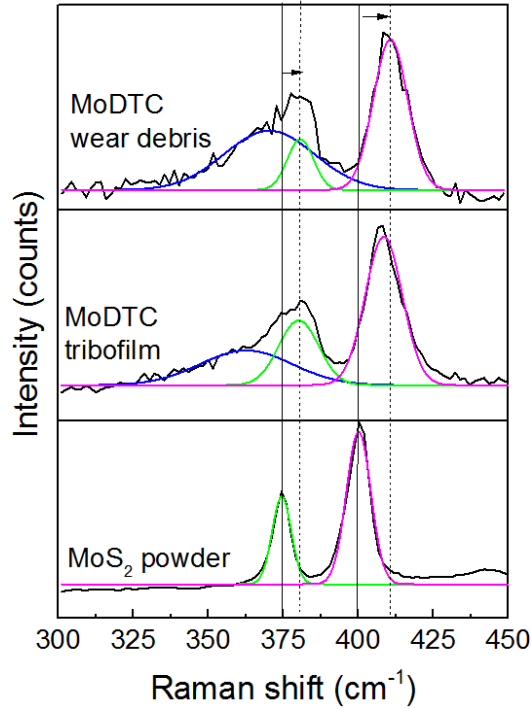


Figure 13. Raman spectra showing MoS<sub>2</sub> first-order peaks due to E<sub>2g</sub><sup>1</sup> and A<sub>1g</sub> modes. All Spectra obtained were at 1 mW laser power, 1s exposure time, 20 accumulations. The spectra are plotted on different scales and are shifted vertically for clarity.

Table 2. MoS<sub>2</sub> Raman peak information

Sample	E <sub>2g</sub> <sup>1</sup> peak frequency (cm <sup>-1</sup> )	E <sub>2g</sub> <sup>1</sup> peak width (cm <sup>-1</sup> )	A <sub>1g</sub> peak frequency (cm <sup>-1</sup> )	A <sub>1g</sub> peak width (cm <sup>-1</sup> )
MoS <sub>2</sub> powder	374.5	6.7	400.3	8.5
MoDTC tribofilm (disc)	379.6	14.3	408.3	13.3
MoDTC wear debris	381.1	10.6	410.8	13.3

It should be noted that for Raman spectra obtained under similar acquisition parameters it was observed that the intensity of both MoS<sub>2</sub> peaks was about 10 times higher in MoS<sub>2</sub> microcrystalline powder than in MoDTC tribofilm. The large difference in intensity can be attributed to the highly crystalline nature of the MoS<sub>2</sub> powder compared to MoS<sub>2</sub> in the tribofilm. MoS<sub>2</sub> peaks of the tribofilm and wear debris are shifted to higher wavenumbers compared to MoS<sub>2</sub> powder by about 8 cm<sup>-1</sup>. The presence of MoS<sub>2</sub> peaks at lower wavenumbers in the powder than in the tribofilm can be attributed to the high laser power



used to acquire the spectra. As mentioned earlier in section 3.1.2, MoS<sub>2</sub> peaks of MoS<sub>2</sub> powder shift to lower wavenumbers with increase in laser power while MoS<sub>2</sub> peaks in MoDTC tribofilms are only slightly affected. At a lower laser power of 0.05 mW, the A<sub>1g</sub> and E<sup>1</sup><sub>2g</sub> peaks of MoS<sub>2</sub> powder were observed at 407 cm<sup>-1</sup> and 382 cm<sup>-1</sup>, respectively. It can thus be seen that at lower laser powers, the position of MoS<sub>2</sub> peaks in MoS<sub>2</sub> powder are similar to those in MoDTC tribofilms at 1 mW laser power. It was also observed that MoS<sub>2</sub> peaks in the tribofilms are broader than those in MoS<sub>2</sub> powder. In MoS<sub>2</sub> powder, the A<sub>1g</sub> peak is broader than the E<sup>1</sup><sub>2g</sub> peak while in the tribofilms the E<sup>1</sup><sub>2g</sub> peak is broader than the A<sub>1g</sub> peak. Broadening of the E<sup>1</sup><sub>2g</sub> peaks is indicative of slight disorder in arrangement of Mo and S atoms in the x-y plane [26,45]. Broadening of the A<sub>1g</sub> peaks can also be due to disorder in the z-axis induced by stress during tribological tests. The influence of tribological processes on the crystal structure of MoS<sub>2</sub> is discussed in section 3.4.2 below.

### 3.4.2 Influence of tribological processes on MoS<sub>2</sub> Raman peaks

Analysis of MoS<sub>2</sub> peaks in MoDTC tribofilms revealed that they were broader compared to microcrystalline MoS<sub>2</sub> powder. Broadening of these peaks was considered to be due to stress-induced disorder in MoS<sub>2</sub> crystal structure during tribological tests. To verify this assumption, tribotests on steel discs with MoS<sub>2</sub> coatings were conducted. The coatings were prepared by first coating the disc with a thin layer of phenolic resin to improve the adherence properties of the surface. The discs were then sprayed with a solution containing MoS<sub>2</sub> in a solvent solution. The solvent in the sprayed discs was then “flash off” by heating the coatings at 120°C for 10 mins before curing them at 200°C for 1h. The coating thickness was 20 μm.

Figure 14 (a) shows the spectrum obtained from the as-prepared coating. MoS<sub>2</sub> Raman peaks are observed at 284 cm<sup>-1</sup> (E<sub>1g</sub>), 382 cm<sup>-1</sup> (E<sup>1</sup><sub>2g</sub>), 407 cm<sup>-1</sup> (A<sub>1g</sub>) and 448 cm<sup>-1</sup> (LA(M)). Tribotests were conducted in the ball-on-disc tribometer by rubbing uncoated steel balls against MoS<sub>2</sub> coated discs under a load of 206 N, 200 rpm rotating speed at room temperature for 30 min. Figure 14 (b) and (c) shows the spectra obtained from the wear scars on the ball and disc. MoS<sub>2</sub> peaks are observed in both spectra although slight differences were observed when compared to spectra from the as-prepared MoS<sub>2</sub> coating. Firstly, there was a broad peak in the region 150 cm<sup>-1</sup> to 250 cm<sup>-1</sup> which was not present in the as-prepared coatings. Secondly, peaks due to formation of graphitic carbon are observed at higher wavenumbers. Thirdly, the intensities of MoS<sub>2</sub> peaks in spectra obtained from the wear scars were less intense compared to the as-prepared MoS<sub>2</sub> coating. Lastly, MoS<sub>2</sub> peaks from the wear scars

were broader compared to the as-prepared coating. The full width at half maxima (FWHM) of the  $A_{1g}$  peak increased by  $10\text{ cm}^{-1}$  after tribotests. Furthermore, the  $E_{2g}^1$  peak was asymmetrical and was properly fitted with two Gaussian curves as shown in Figure 15 (b).

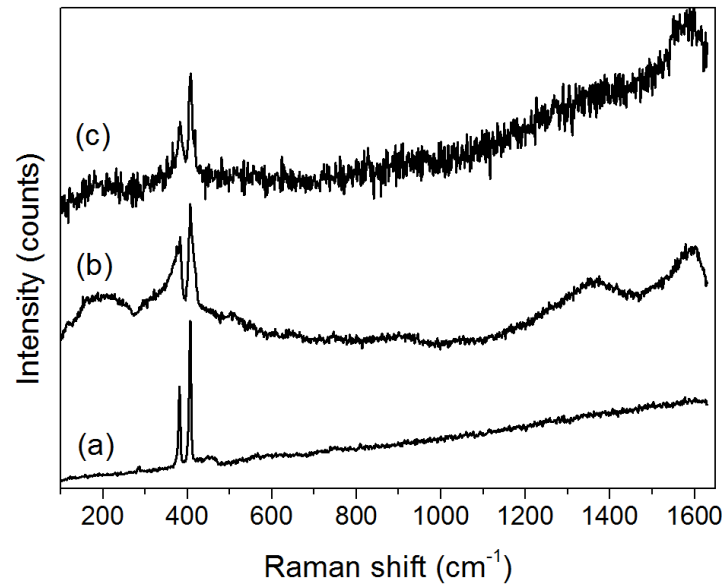


Figure 14. Raman spectra of (a) as-prepared  $\text{MoS}_2$  coating (b) transferred  $\text{MoS}_2$  coating on the ball wear scar (c)  $\text{MoS}_2$  coating on the disc wear scar. The spectra are plotted on different scales and have been shifted for clarity.

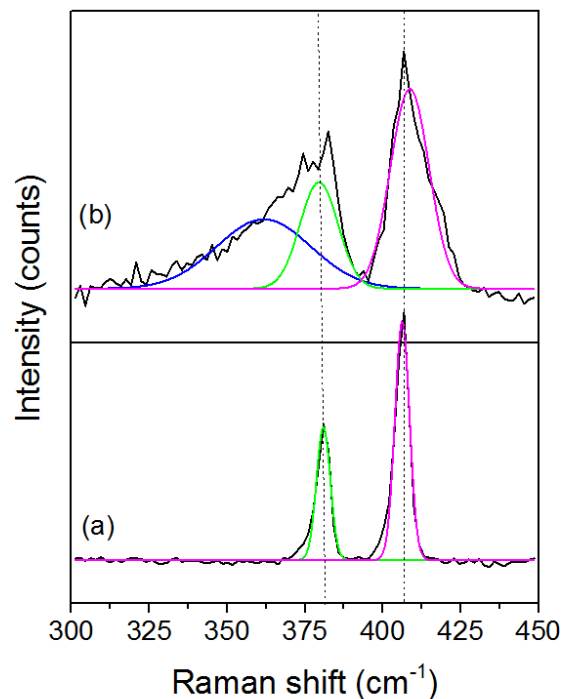


Figure 15. Raman spectra showing the  $E_{2g}^1$  and  $A_{1g}$   $\text{MoS}_2$  peaks of (a) as-prepared  $\text{MoS}_2$  coating and (b) transferred  $\text{MoS}_2$  coating on the ball. All Spectra were obtained at 1 mW laser power, 1s exposure time, 20 accumulations

The broad peak at  $200\text{ cm}^{-1}$  observed after tribotests on the coatings was also observed in spectra obtained from MoDTC tribofilms. This confirms that stress during tribological tests induced disorder in MoS<sub>2</sub> crystal structure in the MoS<sub>2</sub> coatings and MoS<sub>2</sub> in MoDTC tribofilms. The asymmetry observed in the E<sup>1</sup><sub>2g</sub> peak in the MoS<sub>2</sub> coating after tribological tests was similar to that observed in MoDTC tribofilms confirming that the crystal structure of MoS<sub>2</sub> changes when subjected to tribological processes. Broadening of the MoS<sub>2</sub> peaks after tribotests on the MoS<sub>2</sub> coatings also indicate that the broad MoS<sub>2</sub> peaks in MoDTC tribofilms could be as a result of stress-induced disorder in the crystal structure of MoS<sub>2</sub> formed in the tribofilm.

### **3.4.3 MoS<sub>2</sub> formed from thermal decomposition of MoDTC lubricant**

MoS<sub>2</sub> in the MoDTC tribofilms was subjected to stress-induced disorder which altered its crystal structure as was evidenced by the asymmetry of the E<sup>1</sup><sub>2g</sub> peaks and the presence of the broad peak at  $200\text{ cm}^{-1}$ . It was therefore of interest to investigate the crystal structure of MoS<sub>2</sub> formed as a result of MoDTC decomposition but had not been subjected to tribological processes. To do this 5 wt% Fe<sub>3</sub>O<sub>4</sub> was added to 0.6 wt% MoDTC lubricant and the mixture was heated at 100°C for 1h. Fe<sub>3</sub>O<sub>4</sub> was added to the lubricant so as to facilitate decomposition of MoDTC at a lower temperature 100°C similar to that in that the tribotests. Ordinarily, MoDTC decomposes to form MoS<sub>2</sub> at temperatures above 300°C. The other reason for decomposing MoDTC in the presence of iron oxide was because it was observed that iron oxides were formed in the initial stages of rubbing with MoDTC lubricant. After heating the lubricant mixture for 1h, the resulting solid particles were analysed using Raman spectroscopy.

MoS<sub>2</sub> Raman peaks were observed in spectra obtained from the solid particles indicating that MoDTC had decomposed to form MoS<sub>2</sub>. MoS<sub>2</sub> peaks from the solid particles were compared to those obtained from MoDTC tribofilms and microcrystalline MoS<sub>2</sub> powder as shown in Figure 16. MoS<sub>2</sub> formed from thermal decomposition of MoDTC has peaks which are very symmetrical, similar to those of the microcrystalline powder although they are broader. Broadness of the peaks indicates that MoS<sub>2</sub> from the thermal decomposition has low crystallinity compared to the microcrystalline MoS<sub>2</sub> powder. The broad MoS<sub>2</sub> peaks observed in MoDTC tribofilms can be attributed to formation of less crystalline MoS<sub>2</sub> from the decomposition of MoDTC. Further broadening of the MoS<sub>2</sub> peaks occur during tribological tests as was shown in Figure 15. Compared to MoS<sub>2</sub> peaks from thermal decomposition of

MoDTC, MoS<sub>2</sub> peaks in the tribofilm are slightly shifted to higher wavenumbers and the E<sub>2g</sub><sup>1</sup> peak has become asymmetrical. If we consider that MoDTC first decomposes to form MoS<sub>2</sub> within the tribocontact then we can attribute the asymmetry of the E<sub>2g</sub><sup>1</sup> peak to tribological processes.

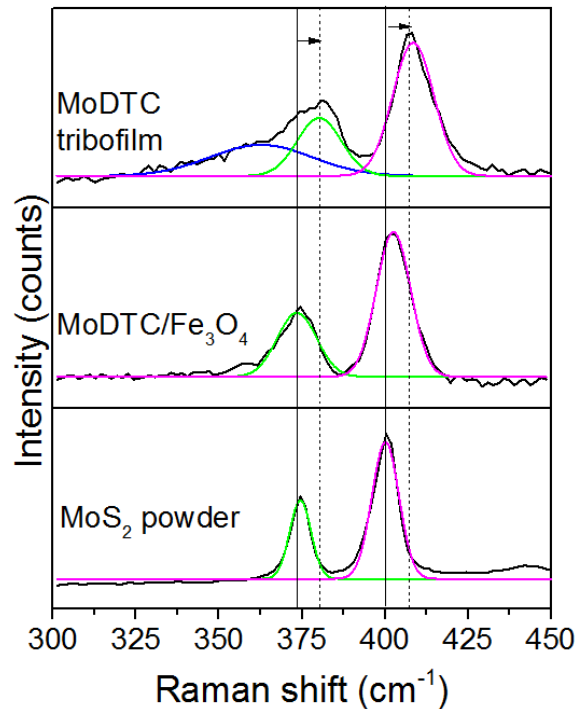


Figure 16. Comparison of MoS<sub>2</sub> formed from thermal and tribological decomposition of MoDTC. All Spectra were obtained at 1 mW laser power, 1s exposure time, 20 accumulations

## 4 Discussion

### 4.1 Influence of laser power on MoDTC tribofilms

At high laser powers, peaks assigned to the formation of haematite (Fe<sub>2</sub>O<sub>3</sub>) were observed in spectra obtained from MoDTC tribofilms. When the exposure time was increased at high laser powers, these iron oxide peaks became more intense. MoO<sub>3</sub>, MoO<sub>2</sub> or molybdenum oxysulphide (MoS<sub>2-x</sub>O<sub>x</sub>) peaks were not observed even at longer exposure times. In preliminary tests conducted without MoDTC additive, under dry friction and mineral base oil, it was observed that haematite and magnetite (Fe<sub>3</sub>O<sub>4</sub>) were present in the wear scars. Raman spectra of the unrubbed steel disc surface showed the presence of iron oxide although at a lower concentration compared to that observed after tests under dry friction or in mineral base oil. Formation of iron oxides in dry friction occurs when rubbing exposes Fe atoms on

the steel surface to atmospheric air resulting in oxidation due to high flash temperatures at the contact. The same process occurs when only the mineral oil is used. In this case, dissolved air in the mineral oil reacts with the nascent surface to form iron oxides. When rubbing in MoDTC lubricant, iron oxides are also formed in the wear scars in the initial stages of the rubbing process. Further rubbing causes iron/iron oxide from the steel surface to be ejected from the surface and subsequently embedded within the growing MoDTC tribofilm. The growth of the tribofilm inhibits the further oxidation of the ferrous surface resulting in a lower concentration of iron oxides in the tribofilm. This explains the absence of iron oxide peaks at low laser powers in wear scar generated using MoDTC lubricant. Generated MoDTC tribofilms are composed of Fe embedded within the organic matrix. Irradiation of the tribofilms at high laser powers causes the iron particles to react with atmospheric air forming iron oxide as evidenced by the formation of dark spots within the tribofilm.

The discussion above explains why  $\text{Fe}_2\text{O}_3$  is observed at high laser power but does not explain why  $\text{MoS}_2$  in the tribofilm is not partially oxidised to  $\text{MoO}_3$  at high laser powers. Windom et al. [24] observed that natural  $\text{MoS}_2$  crystal did not partially oxidise to form  $\text{MoO}_3$  even at high laser powers while  $\text{MoS}_2$  microcrystalline powder oxidised easily. They attributed the lack of  $\text{MoS}_2$  oxidation of the natural crystal to the orientation of the analysed surface. In the case of the natural crystal, the analysed surface was cleaved along the z-axis and did not have its polar edge sites available for oxidation. One explanation for the lack of oxidation of  $\text{MoS}_2$  in the MoDTC tribofilms is that  $\text{MoS}_2$  nanocrystals are orientated along the z-axis in the tribofilm and as such the polar edges are unavailable for oxidation. Another possible explanation for this lack of oxidation could be due the fact that  $\text{MoS}_2$  is present in an organic matrix in the tribofilm which shields  $\text{MoS}_2$  polar edges from oxidation.

#### **4.2 The influence of temperature in the decomposition of MoDTC in a sliding contact**

It has been shown that thermo-oxidative decomposition of MoDTC occurs in two stages: In stage 1, which occurs between 200°C and 300°C, there is elimination of olefins; in stage 2, which occurs around 370°C there is evolution of  $\text{CS}_2$  and  $\text{H}_2\text{S}$  and the formation of  $\text{MoS}_2$  [46,47]. At higher temperatures (420°C),  $\text{MoO}_3$  is formed [46]. The bulk temperature of the lubricants during tribotests was lower than the temperature at which MoDTC decomposes to form  $\text{MoS}_2$ . It is therefore believed that mechanical activation at the asperity-asperity contact provides the remaining energy for the decomposition of MoDTC. Results from this study

show that in a sliding contact, MoDTC decomposed to form MoS<sub>2</sub> at high test temperatures of 100°C whereas at low test temperatures of 40°C the additive decomposed to form molybdenum oxide species, MoS<sub>2</sub> and amorphous sulphur-rich molybdenum (MoS<sub>x</sub>) species. Mechanical activation was the same in tests carried at low and high temperatures since contact parameters were similar. The difference in MoDTC decomposition can therefore be attributed to the bulk temperature.

## 5 Conclusions

Observations from this study are summarised as follows.

- Raman analysis of MoDTC tribofilm reveals that the tribofilms are composed of MoS<sub>2</sub>. Spectra of MoDTC tribofilms obtained with the 488 nm laser shows distinct MoS<sub>2</sub> peaks. Spectra obtained with the 785 nm wavelength laser have a high background which obscures the MoS<sub>2</sub> peaks. The 488 nm laser is therefore more suitable for characterisation of MoDTC tribofilms.
- Spectra acquisition at higher laser powers and longer exposure times causes laser damage to samples and dark spots are observed after analysis. Laser damage results in additional iron oxide peaks being observed in MoDTC tribofilms. In MoS<sub>2</sub> microcrystalline powder, laser damage causes MoO<sub>3</sub> peaks to be observed due to partial oxidation of MoS<sub>2</sub>. Proper care should be taken with regard to laser power and exposure times when obtaining spectra from MoDTC tribofilms to avoid misinterpretation of the spectra.
- During tests conducted with MoDTC lubricant at high temperatures it has been shown that initially iron oxides are formed in the wear scar and high friction is observed. At longer rubbing times MoS<sub>2</sub> is formed at the tribocontact and low friction is obtained. In addition to MoS<sub>2</sub>, amorphous carbon was also formed in the wear scar. No additional chemical species were formed in wear scar due to prolonged rubbing. Spectra from wear debris showed that they were mainly composed of MoS<sub>2</sub>.
- During tribological tests using MoDTC lubricant, high temperatures are necessary for the decomposition of MoDTC to MoS<sub>2</sub> which in turn results in friction reduction. At lower temperatures, MoDTC decomposes to form molybdenum

oxide species, MoS<sub>2</sub> and amorphous sulphur-rich molybdenum (MoS<sub>x</sub>) and as a result there is minimal friction reduction.

- MoS<sub>2</sub> peaks in MoDTC tribofilms and wear debris are asymmetrical and broader compared to MoS<sub>2</sub> microcrystalline powder. Peak asymmetry and broadness are probably due to stress-induced disorder in MoS<sub>2</sub> crystal structure during tribotests.

## 6 Acknowledgement

The authors would like to thank Morris Owen from Everlube Products (UK) for preparing the MoS<sub>2</sub> coatings. This study was funded by the FP7 program through the Marie Curie Initial Training Network (MC-ITN) entitled “ENTICE - Engineering Tribochemistry and Interfaces with a Focus on the Internal Combustion Engine” [290077] and was carried out at University of Leeds, UK.

## 7 Conflict of interest

The authors declare that they have no conflict of interest.

## 8 References

1. Holmberg, K., Andersson, P., Erdemir, A.: Global energy consumption due to friction in passenger cars. *Tribology International* **47**(0), 221-234 (2012). doi:<http://dx.doi.org/10.1016/j.triboint.2011.11.022>
2. Taylor, R.I., Coy, R.C.: Improved fuel efficiency by lubricant design: A review. *Proceedings of the Institution of Mechanical Engineers, Part J: Journal of Engineering Tribology* **214**(1), 1-15 (2000). doi:[10.1177/135065010021400101](https://doi.org/10.1177/135065010021400101)
3. Grossiord, C., Varlot, K., Martin, J.M., Le Mogne, T., Esnouf, C., Inoue, K.: MoS<sub>2</sub> single sheet lubrication by molybdenum dithiocarbamate. *Tribology International* **31**(12), 737-743 (1998).
4. Onodera, T., Morita, Y., Nagumo, R., Miura, R., Suzuki, A., Tsuboi, H., Hatakeyama, N., Endou, A., Takaba, H., Dassenoy, F., Minfray, C., Joly-Pottuz, L., Kubo, M., Martin, J.-M., Miyamoto, A.: A Computational Chemistry Study on Friction of h-MoS<sub>2</sub>. Part II. Friction Anisotropy. *The Journal of Physical Chemistry B* **114**(48), 15832-15838 (2010). doi:[10.1021/jp1064775](https://doi.org/10.1021/jp1064775)
5. Morina, A., Neville, A., Priest, M., Green, J.H.: ZDDP and MoDTC interactions and their effect on tribological performance - Tribofilm characteristics and its evolution. *Tribology Letters* **24**(3), 243-256 (2006).
6. Morina, A., Neville, A., Priest, M., Green, J.H.: ZDDP and MoDTC interactions in boundary lubrication—The effect of temperature and ZDDP/MoDTC ratio. *Tribology International* **39**(12), 1545-1557 (2006). doi:[10.1016/j.triboint.2006.03.001](https://doi.org/10.1016/j.triboint.2006.03.001)
7. Muraki, M., Wada, H.: Influence of the alkyl group of zinc dialkyldithiophosphate on the frictional characteristics of molybdenum dialkyldithiocarbamate under sliding conditions. *Tribology International* **35**(12), 857-863 (2002). doi:[http://dx.doi.org/10.1016/S0301-679X\(02\)00092-0](http://dx.doi.org/10.1016/S0301-679X(02)00092-0)
8. Muraki, M., Yanagi, Y., Sakaguchi, K.: Synergistic effect on frictional characteristics under rolling-sliding conditions due to a combination of molybdenum dialkyldithiocarbamate and zinc dialkyldithiophosphate. *Tribology International* **30**(1), 69-75 (1997). doi:[http://dx.doi.org/10.1016/0301-679X\(96\)00025-4](http://dx.doi.org/10.1016/0301-679X(96)00025-4)
9. Graham, J., Spikes, H., Korcek, S.: The friction reducing properties of molybdenum dialkyldithiocarbamate additives: Part I - Factors influencing friction reduction. *Tribology Transactions* **44**(4), 626-636 (2001).

10. Graham, J., Spikes, H., Jensen, R.: The friction reducing properties of molybdenum dialkyldithiocarbamate additives: Part II - Durability of friction reducing capability. *Tribology Transactions* **44**(4), 637-647 (2001).
11. Grossiord, C., Martin, J.M., Le Mogne, T., Inoue, K., Igarashi, J.: Friction-reducing mechanisms of molybdenum dithiocarbamate/zinc dithiophosphate combination: New insights in MoS<sub>2</sub> genesis. *Journal of Vacuum Science and Technology A: Vacuum, Surfaces and Films* **17**(3), 884-890 (1999).
12. Yamamoto, Y., Gondo, S.: Friction and Wear Characteristics of Molybdenum Dithiocarbamate and Molybdenum Dithiophosphate. *Tribology Transactions* **32**(2), 251-257 (1989). doi:10.1080/10402008908981886
13. Miklozic, K.T., Graham, J., Spikes, H.: Chemical and physical analysis of reaction films formed by molybdenum dialkyl-dithiocarbamate friction modifier additive using Raman and atomic force microscopy. *Tribology Letters* **11**(2), 71-81 (2001).
14. Dickinson, R.G., Pauling, L.: The crystal structure of molybdenite. *Journal of the American Chemical Society* **45**(6), 1466-1471 (1923). doi:10.1021/ja01659a020
15. Onodera, T., Morita, Y., Suzuki, A., Koyama, M., Tsuboi, H., Hatakeyama, N., Endou, A., Takaba, H., Kubo, M., Dassenoy, F., Minfray, C., Joly-Pottuz, L., Martin, J.-M., Miyamoto, A.: A Computational Chemistry Study on Friction of h-MoS<sub>2</sub>. Part I. Mechanism of Single Sheet Lubrication. *The Journal of Physical Chemistry B* **113**(52), 16526-16536 (2009). doi:10.1021/jp9069866
16. Verble, J.L., Wieting, T.J.: Lattice Mode Degeneracy in MoS<sub>2</sub> and Other Layer Compounds. *Physical Review Letters* **25**(6), 362-365 (1970).
17. Wieting, T.J.: Long-wavelength lattice vibrations of MoS<sub>2</sub> and GaSe. *Solid State Communications* **12**(9), 931-935 (1973). doi:http://dx.doi.org/10.1016/0038-1098(73)90111-7
18. Chen, J.M., Wang, C.S.: Second order Raman spectrum of MoS<sub>2</sub>. *Solid State Communications* **14**(9), 857-860 (1974). doi:http://dx.doi.org/10.1016/0038-1098(74)90150-1
19. Wieting, T.J., Verble, J.L.: Infrared and Raman Studies of Long-Wavelength Optical Phonons in Hexagonal MoS<sub>2</sub>. *Physical Review B* **3**(12), 4286-4292 (1971).
20. Wang, Y., Cong, C., Qiu, C., Yu, T.: Raman Spectroscopy Study of Lattice Vibration and Crystallographic Orientation of Monolayer MoS<sub>2</sub> under Uniaxial Strain. *Small* **9**(17), 2857-2861 (2013). doi:10.1002/sml.201202876
21. Evans, B.L., Young, P.A.: Optical Absorption and Dispersion in Molybdenum Disulphide. *Proceedings of the Royal Society of London. Series A, Mathematical and Physical Sciences* **284**(1398), 402-422 (1965). doi:10.2307/2414987
22. Frey, G.L., Tenne, R., Matthews, M.J., Dresselhaus, M.S., Dresselhaus, G.: Raman and resonance Raman investigation of MoS<sub>2</sub> nanoparticles. *Physical Review B* **60**(4), 2883-2892 (1999).
23. Zeng, H., Zhu, B., Liu, K., Fan, J., Cui, X., Zhang, Q.M.: Low-frequency Raman modes and electronic excitations in atomically thin MoS<sub>2</sub> films. *Physical Review B* **86**(24), 241301 (2012).
24. Windom, B., Sawyer, W.G., Hahn, D.: A Raman Spectroscopic Study of MoS<sub>2</sub> and MoO<sub>3</sub>: Applications to Tribological Systems. *Tribology Letters* **42**(3), 301-310 (2011). doi:10.1007/s11249-011-9774-x
25. Stacy, A.M., Hodul, D.T.: Raman spectra of IVB and VIB transition metal disulfides using laser energies near the absorption edges. *Journal of Physics and Chemistry of Solids* **46**(4), 405-409 (1985). doi:http://dx.doi.org/10.1016/0022-3697(85)90103-9
26. McDevitt, N.T., Zabinski, J.S., Donley, M.S., Bultman, J.E.: Disorder-Induced Low-Frequency Raman Band Observed in Deposited MoS<sub>2</sub> Films. *Appl. Spectrosc.* **48**(6), 733-736 (1994).
27. Luo, X., Zhao, Y., Zhang, J., Xiong, Q., Quek, S.Y.: Anomalous frequency trends in MoS<sub>2</sub> thin films attributed to surface effects. *Physical Review B* **88**(7), 075320 (2013).
28. Lee, C., Yan, H., Brus, L.E., Heinz, T.F., Hone, J., Ryu, S.: Anomalous Lattice Vibrations of Single- and Few-Layer MoS<sub>2</sub>. *ACS Nano* **4**(5), 2695-2700 (2010). doi:10.1021/nn1003937
29. Li, H., Zhang, Q., Yap, C.C.R., Tay, B.K., Edwin, T.H.T., Olivier, A., Baillargeat, D.: From Bulk to Monolayer MoS<sub>2</sub>: Evolution of Raman Scattering. *Advanced Functional Materials* **22**(7), 1385-1390 (2012). doi:10.1002/adfm.201102111



30. Chakraborty, B., Matte, H.S.S.R., Sood, A.K., Rao, C.N.R.: Layer-dependent resonant Raman scattering of a few layer MoS<sub>2</sub>. *Journal of Raman Spectroscopy* **44**(1), 92-96 (2013). doi:10.1002/jrs.4147
31. Bagnall, A.G., Liang, W.Y., Marseglia, E.A., Welber, B.: Raman studies of MoS<sub>2</sub> at high pressure. *Physica B+C* **99**(1-4), 343-346 (1980). doi:http://dx.doi.org/10.1016/0378-4363(80)90257-0
32. Livneh, T., Sterer, E.: Resonant Raman scattering at exciton states tuned by pressure and temperature in 2H-MoS<sub>2</sub>. *Physical Review B* **81**(19), 195209 (2010).
33. Sugai, S., Ueda, T.: High-pressure Raman spectroscopy in the layered materials 2H-MoS<sub>2</sub>, 2H-MoSe<sub>2</sub>, and 2H-MoTe<sub>2</sub>. *Physical Review B* **26**(12), 6554-6558 (1982).
34. Sahoo, S., Gaur, A.P.S., Ahmadi, M., Guinel, M.J.F., Katiyar, R.S.: Temperature-Dependent Raman Studies and Thermal Conductivity of Few-Layer MoS<sub>2</sub>. *The Journal of Physical Chemistry C* **117**(17), 9042-9047 (2013). doi:10.1021/jp402509w
35. Thripuranthaka, M., Kashid, R.V., Sekhar Rout, C., Late, D.J.: Temperature dependent Raman spectroscopy of chemically derived few layer MoS<sub>2</sub> and WS<sub>2</sub> nanosheets. *Applied Physics Letters* **104**(8), - (2014). doi:doi:http://dx.doi.org/10.1063/1.4866782
36. Najmaei, S., Ajayan, P.M., Lou, J.: Quantitative analysis of the temperature dependency in Raman active vibrational modes of molybdenum disulfide atomic layers. *Nanoscale* **5**(20), 9758-9763 (2013). doi:10.1039/c3nr02567e
37. Lanzillo, N.A., Glen Birdwell, A., Amani, M., Crowne, F.J., Shah, P.B., Najmaei, S., Liu, Z., Ajayan, P.M., Lou, J., Dubey, M., Nayak, S.K., apos, Regan, T.P.: Temperature-dependent phonon shifts in monolayer MoS<sub>2</sub>. *Applied Physics Letters* **103**(9), - (2013). doi:doi:http://dx.doi.org/10.1063/1.4819337
38. Su, L., Zhang, Y., Yu, Y., Cao, L.: Dependence of coupling of quasi 2-D MoS<sub>2</sub> with substrates on substrate types, probed by temperature dependent Raman scattering. *Nanoscale* **6**(9), 4920-4927 (2014). doi:10.1039/c3nr06462j
39. Najmaei, S., Liu, Z., Ajayan, P.M., Lou, J.: Thermal effects on the characteristic Raman spectrum of molybdenum disulfide (MoS<sub>2</sub>) of varying thicknesses. *Applied Physics Letters* **100**(1), - (2012). doi:doi:http://dx.doi.org/10.1063/1.3673907
40. Willermet, P.A., Carter, R.O., Schmitz, P.J., Everson, M., Scholl, D.J., Weber, W.H.: Formation, structure, and properties of lubricant-derived antiwear films. *Lubrication Science* **9**(4), 325-348 (1997).
41. Colomban, P., Cherifi, S., Despert, G.: Raman identification of corrosion products on automotive galvanized steel sheets. *Journal of Raman Spectroscopy* **39**(7), 881-886 (2008).
42. Zabinski, J.S., MacDevitt, N.T.: Raman spectra of inorganic compounds related to solid state tribochemical studies. In. USAF Wright Laboratory Report No. WL-TR-96-4034, (1996)
43. Weber, T., Muijsers, J.C., Niemantsverdriet, J.W.: Structure of Amorphous MoS<sub>3</sub>. *The Journal of Physical Chemistry* **99**(22), 9194-9200 (1995). doi:10.1021/j100022a037
44. Wang, T., Zhuo, J., Du, K., Chen, B., Zhu, Z., Shao, Y., Li, M.: Electrochemically Fabricated Polypyrrole and MoS<sub>x</sub> Copolymer Films as a Highly Active Hydrogen Evolution Electrocatalyst. *Advanced Materials* **26**(22), 3761-3766 (2014). doi:10.1002/adma.201400265
45. McDevitt, N.T., Zabinski, J.S., Donley, M.S.: The use of Raman scattering to study disorder in pulsed laser deposited MoS<sub>2</sub> films. *Thin Solid Films* **240**(1-2), 76-81 (1994). doi:http://dx.doi.org/10.1016/0040-6090(94)90698-X
46. Isoyama, H., Sakurai, T.: The lubricating mechanism of di-μ-thio-dithio-bis (diethyldithiocarbamate) dimolybdenum during extreme pressure lubrication. *Tribology* **7**(4), 151-160 (1974). doi:http://dx.doi.org/10.1016/0041-2678(74)90022-0
47. Sakurai, T., Okabe, H., Isoyama, H.: The Synthesis of Di-μ-thio-dithio-bis (dialkyldithiocarbamates) Dimolybdenum (V) and Their Effects on Boundary Lubrication. *Bulletin of The Japan Petroleum Institute* **13**(2), 243-249 (1971). doi:10.1627/jpi1959.13.243